PHYSICO-CHEMICAL STUDIES OF SUPERCOOLED LIQUIDS

THESIS SUBMITTED
IN FULFILMENT OF THE REQUIREMENTS
FOR
THE DEGREE OF DOCTOR OF PHILOSOPHY
IN CHEMISTRY

BY
MD. RAFIQUL ISLAM

DEPARTMENT OF CHEMISTRY
ALIGARH MUSLIM UNIVERSITY
ALIGARH
1973

T.1229

A B S T R A C T

Electrical conductances of tetra-n-butylammonium halide and those of their mixtures with manganese(II) chloride have been measured as functions of temperature and composition. The metal halide-rich mixture with $n\text{-}(C_4H_9)_4NX$ (X=Cl, Br, I) have been found to supercool to glassy materials. The capacitance of the electrical double layer (electrode-electrolyte) have been found to be of the order of $(3\text{-}6) \times 10^{-4}$ pf, in the glassy material and therefore has insignificant effect on the measured conductances. Similarly, such measurements have been made with $CoCl_2$ + $n\text{-}(C_4H_9)_4NI$, and the glassy states of MCl_2 (M=Mn, Co and Ni) + $n\text{-}(C_4H_9)_4NCl$. These data have been analysed in terms of different functional forms by computing the parameters on computer IBM1130. The decrease in conductance with an increase in the metal ion concentration has been interpreted in terms of complex formation. This has been supported by the charge-transfer and the ligand-field transition spectra for the tetrahedral symmetry of the complex ions in thin films of the glassy state. The glass forming tendency has been interpreted in terms of the ideal glass transition temperature T_o, dependence of activation energy on temperature, large cation-to-anion ratio, decrease of configurational entropy, increased intermolecular forces and the decrease of free volume which freezes the mobility of the ions.

Department of Chemistry
Aligarh Muslim University
Aligarh

This is to certify that the thesis entitled 'Physico-Chemical Studies of Supercooled Liquids' is the original work carried out by Md. Rafiqul Islam under my supervision and is suitable for submission for the award of Ph.D. degree in Chemistry.

Nurul Islam
M.Sc. (New York)
Reader

ACKNOWLEDGEMENT

The author wishes to express his deep sense of gratitude to Dr. Nurul Islam, Ph.D. (New York) for his unstinted help, valuable guidance and generous attitude during the course of this work, to Professor W. Rahman, Head, Department of Chemistry for providing research facilities and to the C.S.I.R. (New Delhi) for the award of research fellowship.

The author also wishes to thank Dr. Moonis Ali of the Computer Centre, Aligarh Muslim University, for his help in computer programming and all of his research colleagues in the laboratory for their cooperation.

Md. Rafiqul Islam.

Md. Rafiqul Islam

C O N T E N T S

A B S T R A C T

Electrical conductances of tetra-n-butylammonium halide and those of their mixtures with manganese(II) chloride have been measured as functions of temperature and composition. The metal halide-rich mixture with $n\text{-}(C_4H_9)_4NX$ (X=Cl, Br, I) have been found to supercool to glassy materials. The capacitance of the electrical double layer (electrode-electrolyte) have been found to be of the order of (3-6) x 10^{-4} pf, in the glassy material and therefore has insignificant effect on the measured conductances. Similarly, such measurements have been made with $CoCl_2$ + $n\text{-}(C_4H_9)_4NI$, and the glassy states of MCl_2 (M=Mn, Co and Ni) + $n\text{-}(C_4H_9)_4NCl$. These data have been analysed in terms of different functional forms by computing the parameters on computer IBM1130. The decrease in conductance with an increase in the metal ion concentration has been interpreted in terms of complex formation. This has been supported by the charge-transfer and the ligand-field transition spectra for the tetrahedral symmetry of the complex ions in thin films of the glassy states. The glass forming tendency has been interpreted in terms of the ideal glass transition temperature T_0, dependence of activation energy on temperature, large cation-to-anion ratio,

decrease of configurational entropy, increased intermolecular forces and the decrease of free volume which freezes the mobility of the ions.

INTRODUCTION

Although the glass-forming tendency of solute rich mixtures of molten salt systems is not unknown[1], very little has been explored in this area. It has been found[2] in recent years that a large cation-to-anion ratio forces the metal ion to assume almost pure tetrahedral geometry and at the same time facilitates the supercooling of manganese(II)-, iron(III)-, cobalt(II)-, and nickel(II)- halides-rich mixtures of molten tetra-n-butylphosphonium halides to glassy substances[3]. The supercooling of nickel(II) chloride-rich mixtures of molten tri-n-butylbenzyl phosphonium chloride to glassy state has been reported by Pedro Smith and von Winbush[4]. The comparison of the absorption spectra[2] of dilute solutions of the metal halides with those of the corresponding glassy states reveals that the tetrahedral geometry of the metal complex ions remain unaffected by the glass formation.

Gasteal and Hodge[5] considered a solid as one in which the liquid structure has been 'frozen in', the chief characteristic which differentiates the glasses from the liquids being the mobility of the constituent entities.

The transport properties of molten salts have most

frequently been interpreted in terms of the rate process theory. The temperature coefficients of transport processes are obtained in the form of activation energies, however, the rate process theory has not been able to give any clear account of the variation of activation energy with temperature as has been observed particularly with low melting salts and their mixtures.

The present work has been carried out with a view to understanding the differences in dilute solutions (MCl_2 + molten salt solvents; M=Mn, Co, and Ni) and the corresponding glassy states; and also the factors influencing the glass formation. For this purpose, the electrical conductances have been studied as functions of composition and temperature. The effect of capacitance of the electrical double layer has also been taken into account. The mechanism of conductance has been examined in the light of rate process[6-9] and the 'free-volume' theories[10]. The latter theory has been widely employed in explaining the transport behaviour of molten salt systems.

The results have been interpreted in terms of the parameters of the following equations:

$$k = a + bt + ct^2 = a' \exp\left[-b'/(t-c')\right]$$

$$= A_k T^{-\frac{1}{2}} \exp\left[-k'/(T-T_0)\right] \qquad \text{constant composition}$$

$$\Lambda = A_\Lambda T^{-\frac{1}{2}} \exp\left[-k_\Lambda/(T-T_0)\right]$$

where a, b, c, a', b', c', A_k, k', T_0, A_Λ and k_Λ are constants, k and Λ are specific and equivalent conductances, and t(^oC) and T(^oK) stand for the temperatures on the two scales.

$$\Lambda = A'_\Lambda T^{-\frac{1}{2}} \exp\left[-B_\Lambda / R(N_0 - N)\right] \qquad \text{constant temperature}$$

The constants A'_Λ, k_Λ, and B_Λ are characteristic of the transport process and the chemical system; and T_0, R and N_0 are constants of the chemical system alone provided the external pressure is kept constant. R expresses the dependence of T_0 on concentration N.

The importance of the ideal glass transition temperature T_0, dependence of activation energy on temperature, large cation-to-anion ratio, decrease of configurational entropy, increased intermolecular forces and the decrease of free volume have been considered in relation to the glass-forming tendency of the molten salt systems under investigation.

The charge-transfer and the ligand-field transitions have also been studied using thin films of the glassy materials in order to ascertain the geometry of the metal complex ions in these glass-forming systems.

ELECTRICAL CONDUCTANCE AND THE GLASS FORMING TENDENCY OF MOLTEN SALT MIXTURES OF MANGANESE(II) CHLORIDE AND TETRA-n-BUTYLAMMONIUM HALIDE.

Experimental

Chemicals.

Tetra-n-butylammonium-chloride, -bromide (Fluka, Switzerland), and iodide (BDH) were used as solvents in the molten state. The $n\text{-}(C_4H_9)_4NCl$ and $n\text{-}(C_4H_9)_4NBr$ salts being extremely hygroscopic in nature, were handled with extra care in an inert atmosphere. The anhydrous $SnCl_2$ was prepared from the hydrated $SnCl_2$(BDH) by heating at 130°C in an oven and was later stored in a vacuum desiccator.

Instrumentation.

The conductances were measured with a conductivity bridge of WTW (Leitfahigkeitsmesser) type-LBR at a frequency of 50 c/s. The conductivity cell consists of two platinum electrodes connected with two copper wires. The electrodes were made of platinum foils being shielded with two platinum wires. Platinizing of the electrode was not recommended for molten salts as the electrode polarization is not usually significant in such systems. The conductivity cell was calibrated by determining its cell constant (1.0284 cm^{-1}) with a decinormal

solution of potassium chloride in triply distilled water at 25°C. In order to ensure a uniform temperature throughout the measurement the conductivity cell was immersed in a vegetable oil containing jacket fitted with a thermometer and the jacket was immersed in a thermostated oil bath. The thermostated bath consists of an immersion heater, stirrer and a thermometer. The temperature of the bath was controlled with the help of an autotransformer DI-MORSTAT-TYPE-(1633/2353) regulator. The two thermometers gave comparable results throughout the measurement. The autotransformer and the conductivity bridge were supplied with power via voltage stabilizer because of an average fluctuation of ± 5 % in 220 volts supply.

Procedure.

A weighed amount of tetra-n-butylammonium chloride was allowed to melt in a sample tube placed in the jacket of the thermostated bath in an inert atmosphere. The electrodes were immersed in the molten sample whose conductance was measured at several temperatures. Then the cell was removed from the sample tube and kept hanging in an empty tube placed in the desiccator. In the meantime a weighed amount of anhydrous $MnCl_2$ was added to the sample tube containing tetra-n-butylammonium chloride and the mixture was heated in the jacketed

thermostat at $\sim 110^{\circ}C$ for several hours until a clear solution was obtained. The electrodes were replaced to the sample tube and the conductances measured at different temperatures. This process was repeated until a saturated solution was obtained as a glassy material. Similarly, the conductances of pure n-$(C_4H_9)_4NBr$ and n-$(C_4H_9)_4NI$ and those of the several compositions of their mixtures with $MnCl_2$ were measured as a function of temperature. The preparation of the samples as well as the measurements of conductances were carried out under an atmosphere of pure dry nitrogen.

The conductances of the molten samples were measured at intervals of 10° of temperature over a range of 30°-$160^{\circ}C$ for n-$(C_4H_9)_4NCl$ and n-$(C_4H_9)_4NBr$, and those for n-$(C_4H_9)_4NI$ over 27°-160°. The melting points of n-$(C_4H_9)_4NCl$, n-$(C_4H_9)_4NBr$, and n-$(C_4H_9)_4NI$ have been found to be $92 \pm 1^{\circ}$, $116 \pm 0.5^{\circ}$ and $139 \pm 1^{\circ}C$ respectively. The conductance measurements were carried out with an accuracy of about $\pm 0.5 \times 10^{-3}$ ohm^{-1}. The conductivity cell was cleaned with hot distilled water, and soaked overnight in conductivity water and the cell constant was checked after each set of measurement.

The equivalent conductance, Λ, mean equivalent weight, e and equivalent fraction, f were calculated with the help of the expressions given in Appendix A.

RESULTS AND DISCUSSION

The specific and equivalent conductances of pure molten n-$(C_4H_9)_4NX$ (X=Cl, Br, I) and those of their mixtures with $MnCl_2$ have been measured[11]. These measurements were made over 373°-413°K in the cases of pure n-$(C_4H_9)_4NCl$ and its mixtures with $MnCl_2$; those of 21.8, 35.3, 38.6 and 42.0 mole % $MnCl_2$ in n-$(C_4H_9)_4NBr$; and 14.4, 19.9, and 29.8 mole % $MnCl_2$ in n-$(C_4H_9)_4NI$ while over 393-413°K in the cases of n-$(C_4H_9)_4NBr$ and its mixtures with 18.6 and 20 mole % $MnCl_2$; and over 418-433°K in the cases of n-$(C_4H_9)_4NI$ and its mixtures with 4.7 and 9.8 mole % $MnCl_2$. In extremely dilute solutions the measured conductances between 30 and 90°C were not reproducible whereas in solutions of relatively higher concentrations, the results were found to be reproducible above 30°C. However, at temperatures above the melting points, the conductances were reproducible in dilute as well as in relatively more concentrated solutions as expected for the liquid state. The behaviour of dilute solutions below the melting points may apparently be due to poor, non-uniform electrical contacts in the solidified state and as the concentration of $MnCl_2$ increases, the mixture softens and slowly becomes less opaque until finally a transparent glassy material is obtained.

The electrical conductances of molten salts and their

temperature dependence may be correlated to the nature of the conducting species. As may be noted that average increases in conductance for every 10^{0} rise in temperature are 0.09, 0.25 and 0.70 ohm^{-1} cm^{2} $equiv^{-1}$ in the cases of chloride, bromide and iodide respectively. It may presumably suggest an increase in the ion association from iodide through chloride. Thus the chloride being relatively poor conductor due to the high degree of covalency may be considered to have inherent tendency to form associated molecules which may break up into simpler species upon heating.

The conductances at a given temperature were found to increase from chloride through iodide and increase considerably with increase in temperature. These results are in accordance with those reported earlier for similar systems[5,12,13]. This may be attributed to an increase in the free volume[10,14] which increases the ionic mobility with temperature. The concept of free volume theory for the transport behaviour of ionic liquids may be understood in terms of Cohen and Turnbull's model[10]. According to them a constituent particle of a liquid may undergo diffusive displacement when a void above a certain critical size becomes available for a neighbouring molecule to jump into the position vacated by the displacement. This in turn prevents the return of the first particle. The voids presumably arise from the redistribution of the 'free volume' in the liquid structure. The free volume is defined as one which may be redistributed without any energy change.

The conductances have been found to decrease with an increase in the mole fraction of $MnCl_2$ as reported[15] in similar studies. This may be attributed to the removal of more mobile anions, X^- as compared to Bu_4N^+ due to complex formation and a simultaneous decrease in the 'free volume' as will be discussed later. The absorption spectra of such solutions support the formation of tetrahedral complexes as will be considered later. The process of complex formation continues until almost all the solvent anions get tied up to the added metal ion ($\sim$ 33 mole %) and the mixture supercools to a glassy state.

Computation of the parameters.

The specific conductance data of pure $n\text{-}(C_4H_9)_4NX$ (X = Cl, Br, I) and those of their mixtures with anhydrous $MnCl_2$ (Table I) reported earlier[11] have been fitted in several functional forms by the least square method on computer IBM 1130. The typical values of the parameters of different equations for pure $n\text{-}(C_4H_9)_4NX$ (X = Cl, Br, I) and their mixtures with $MnCl_2$ are summarised in Table II. These parameters have been found to be temperature independent, however, they depend on composition. The activation energies for specific conductance, E_κ's have been evaluated over a specified range of temperature from the

TABLE - I

Specific conductances ($Ohm^{-1}cm^{-1}$) as a function of temperature for molten salt systems: A. $MnCl_2$+Bu_4NCl; B. $MnCl_2$+Bu_4NBr; and C. $MnCl_2$+Bu_4NI

A. $MnCl_2$+Bu_4NCl

t(°C)	0 mole % k x 10^3	10.1 mole % k x 10^3	12.7 mole % k x 10^3	15.4 mole % k x 10^3	20.1 mole % k x 10^3	24.6 mole % k x 10^3	28.0 mole % k x 10^3
100	1.430	1.162	1.079	1.079	0.5664	0.3598	0.2982
110	1.650	1.644	1.542	1.439	0.8020	0.5140	0.4730
120	2.108	2.108	2.056	2.056	1.1310	0.7401	0.6160
130	2.467	2.679	2.569	2.673	1.4900	1.0280	0.8020
140	2.776	3.498	3.290	3.392	1.9540	1.3270	1.0070

TABLE - I (Contd.)

B. $MnCl_2$ + Bu_4NBr

t(°C)	0 mole % k x 10^3	18.6 mole % k x 10^3	20.0 mole % k x 10^3	31.8 mole % k x 10^3	35.3 mole % k x 10^3	38.6 mole % k x 10^3	42.0 mole % k' x 10^3
100	-	-	-	0.4470	0.3906	0.3598	0.3290
110	-	-	-	0.6580	0.5757	0.5449	0.5551
120	1.3370	1.9540	1.7990	0.9149	0.8121	0.8020	0.7885
125	1.6979	2.3368	2.2046	1.1085	0.9857	0.9655	0.9581
130	2.0560	2.7240	2.5690	1.3370	1.1820	1.1210	1.1210
135	2.4175	3.1094	2.9988	1.4967	1.3440	1.2974	1.3274
140	2.7760	3.4950	3.1870	1.6440	1.5420	1.4990	1.5420

TABLE - I (Contd.)

C. $MnCl_2$ + Bu_4NI

t(°C)	0 mole % k x 10^3	4.7 mole % k x 10^3	9.6 mole % k x 10^3	14.4 mole % k x 10^3	19.9 mole % k x 10^3	20.5 mole % k x 10^3
100	-	-	-	1.1820	1.0280	0.9149
110	-	-	-	1.7480	1.4390	1.2340
120	-	-	-	2.6730	1.8500	1.9020
130	-	-	-	3.7010	2.9290	2.7240
140	4.1100	5.6030	5.2940	4.6770	3.7530	3.6500
145	5.0433	6.3543	6.0194	-	-	-
150	5.9700	7.1450	6.7840	5.9120	4.7800	4.7300
155	6.8987	7.9732	7.5874	-	-	-
160	7.8200	8.9410	8.4200	7.5040	5.9120	5.8080

TABLE - II

Computer fitted least square representation for specific and equivalent conductances as a function of temperature ($t^{\circ}C$, $T^{\circ}K$) for molten salt systems: A. $MnCl_2$+Bu_4NCl; B. $MnCl_2$+Bu_4NBr and C. $MnCl_2$+Bu_4NI.

A. $MnCl_2$ + Bu_4NCl
(373° - $413^{\circ}K$)

Mole % $MnCl_2$	Eqn.	a	b	c	Stand. Error
0.0	(i)	-0.2833×10^{-2}	0.5002×10^{-4}	-0.0713×10^{-6}	0.03
	(ii)	0.0102	157.1	292.2	0.03
	(iii)	42.95	99.75	315.04	0.01
10.1	(i)	0.1315×10^{-2}	-0.4428×10^{-4}	0.4287×10^{-6}	0.05
	(ii)	0.1963	742.04	228.3	0.05
	(iii)	113.92	208.51	305.17	0.02
12.7	(i)	0.0820×10^{-2}	-0.3427×10^{-4}	0.3695×10^{-6}	0.03
	(ii)	0.10344	573.08	247.12	0.03
	(iii)	124.48	242.25	295.95	0.01
15.4	(i)	0.2309×10^{-2}	-0.6331×10^{-4}	0.5079×10^{-6}	0.03
	(ii)	0.3653	918.63	216.32	0.04
	(iii)	112.14	242.30	295.00	0.05
20.1	(i)	0.1946×10^{-2}	-0.4843×10^{-4}	0.3462×10^{-6}	0.005
	(ii)	0.2436	933.03	219.65	0.009
	(iii)	105.76	312.11	292.67	0.005
24.6	(i)	0.1479×10^{-2}	-0.3692×10^{-4}	0.2566×10^{-6}	0.007
	(ii)	0.15196	857.24	231.80	0.005
	(iii)	256.57	595.75	260.30	0.003
28.0	(i)	-0.0413×10^{-2}	-0.00166×10^{-4}	0.0735×10^{-6}	0.009
	(ii)	0.0691	246.30	300.24	0.01
	(iii)	47.67	311.32	290.7	0.002

(i) $k = a+bt+ct^2$; (ii) $k = a \exp\left[-b/(T-c)\right]$; and (iii) $\Lambda = aT^{1/2} \exp\left[-b/(T-c)\right]$

TABLE - II (Contd.)

B. $MnCl_2$ + Bu_4NBr

(393^0 - 413^0K)

Mole % $MnCl_2$	Eqn.	a	b	c	Stand. Error
0.0	(i)	-0.7215×10^{-2}	0.7069×10^{-4}	0.0049×10^{-6}	0.0
	(ii)	0.0149	110.99	346.94	0.0
	(iii)	95.11	96.79	354.99	0.001
18.6	(i)	-0.7208×10^{-3}	0.7575×10^{-4}	-0.005×10^{-6}	0.0
	(ii)	0.0199	139.29	333.04	0.0
	(iii)	110.68	156.74	330.42	0.0
20.0	(i)	-1.9297×10^{-2}	2.6700×10^{-4}	-0.7599×10^{-6}	0.0
	(ii)	0.0077	44.68	362.20	0.0
	(iii)	32.95	31.79	370.35	0.0

(373^0 - 413^0K)

31.8	(i)	0.0931×10^{-2}	-0.3043×10^{-4}	0.2548×10^{-6}	0.03
	(ii)	0.0195	276.75	300.97	0.03
	(iii)	14.52	72.75	339.86	0.02
35.3	(i)	0.1461×10^{-2}	-0.3941×10^{-4}	0.2855×10^{-6}	0.02
	(ii)	0.0671	549.34	267.45	0.02
	(iii)	23.12	147.85	320.87	0.01
39.6	(i)	0.0794×10^{-2}	-0.2809×10^{-4}	0.2357×10^{-6}	0.01
	(ii)	0.0898	629.57	257.5	0.007
	(iii)	31.78	205.43	310.19	0.009
42.0	(i)	0.2169×10^{-2}	-0.5235×10^{-4}	0.3453×10^{-6}	0.01
	(ii)	0.0267	321.85	300.65	0.02
	(iii)	38.92	266.18	298.15	0.009

(i) $k = a+bt+ct^2$; (ii) $k = a \exp[-b/(T-c)]$; and

(iii) $\Lambda = aT^{1/2} \exp[-b/(T-c)]$.

TABLE - II (Contd.)

C. $MnCl_2$ + Bu_4NI

Mole % $MnCl_2$	Temp. range (°K)		a	b	c	Stand. Error
0.0	413-433	(i)	-2.298×10^{-2}	2.005×10^{-4}	-0.0499×10^{-6}	0.0
		(ii)	0.0419	121.254	360.79	0.0
		(iii)	643.54	206.03	347.96	0.002
4.7	413-433	(i)	0.0179×10^{-2}	-0.6902×10^{-4}	0.7697×10^{-6}	0.0
		(ii)	0.2263	525.81	270.84	0.0
		(iii)	2092.3	610.98	263.11	0.0003
9.6	413-433	(i)	0.0814×10^{-2}	-0.7720×10^{-4}	0.7800×10^{-6}	0.0
		(ii)	0.2144	514.88	273.89	0.0
		(iii)	1859.2	607.98	264.97	0.0002
14.4	373-433	(i)	0.3254×10^{-2}	-0.9931×10^{-4}	0.7844×10^{-6}	0.07
		(ii)	0.2884	657.67	253.09	0.07
		(iii)	330.14	253.3	308.6	0.04
19.9	373-433	(i)	0.4439×10^{-2}	-1.0814×10^{-4}	0.7351×10^{-6}	0.10
		(ii)	0.1546	535.01	269.097	0.10
		(iii)	210.48	237.29	310.67	0.07
20.5	373-433	(i)	0.4030×10^{-2}	-1.0401×10^{-4}	0.7217×10^{-6}	0.06
		(ii)	0.1147	445.46	283.65	0.06
		(iii)	376.93	345.48	296.07	0.04

(i) $k = a+bt+ct^2$; (ii) $k = a \exp[-b/(T-c)]$; and

(iii) $\Lambda = a\bar{I}^{1/2} \exp[-b/(T-c)]$.

derivatives, $[d\ln k/d(T^{-1})]$ of the following analytical expressions based on the free-volume model:

$$k = a + bt + ct^2,$$

$$k = a' \exp[-b'/(T-c')]$$

The average of activation energies thus obtained have been plotted as functions of composition (Fig. 1) and temperature (Fig. 2).

It may be noted from Fig. 1-i that the energy of activation of the pure $n\text{-}(C_4H_9)_4NCl$ has lower value than the corresponding mixtures with $SnCl_2$ unlike those in the bromide (Fig. 1-ii) and iodide (Fig. 1-iii) systems. But as soon as the mixture is formed the E_k's become insensitive to any variation in the composition of the solute. Thus the activation energies for isothermal conductances are apparently independent of composition (Fig. 1). This is exactly what one would expect in the case of fused salt systems. However, the energy of activation decreases with an increase in the temperature of the molten salt systems (Fig. 2). The E_k values are found to increase considerably at low temperatures and decrease slowly with increase in temperature. The variation in activation energy with temperature above the melting point is not very appreciable as the molten salt systems behave like ordinary liquids at relatively higher temperatures. This shows that the Arrhenius type of equation is not suitable

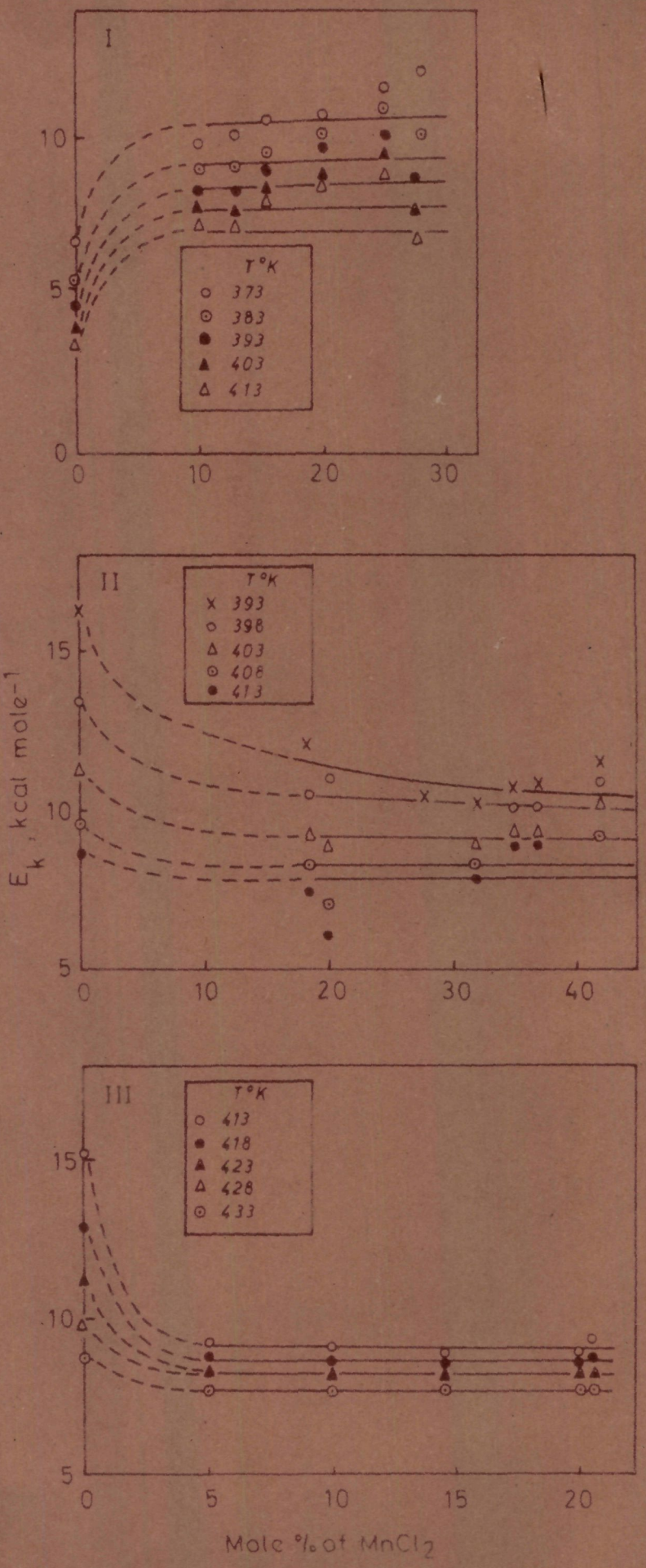

Fig.1 Energy of activation as a function of composition for molten salt systems: (I) $MnCl_2 + Bu_4NCl$,

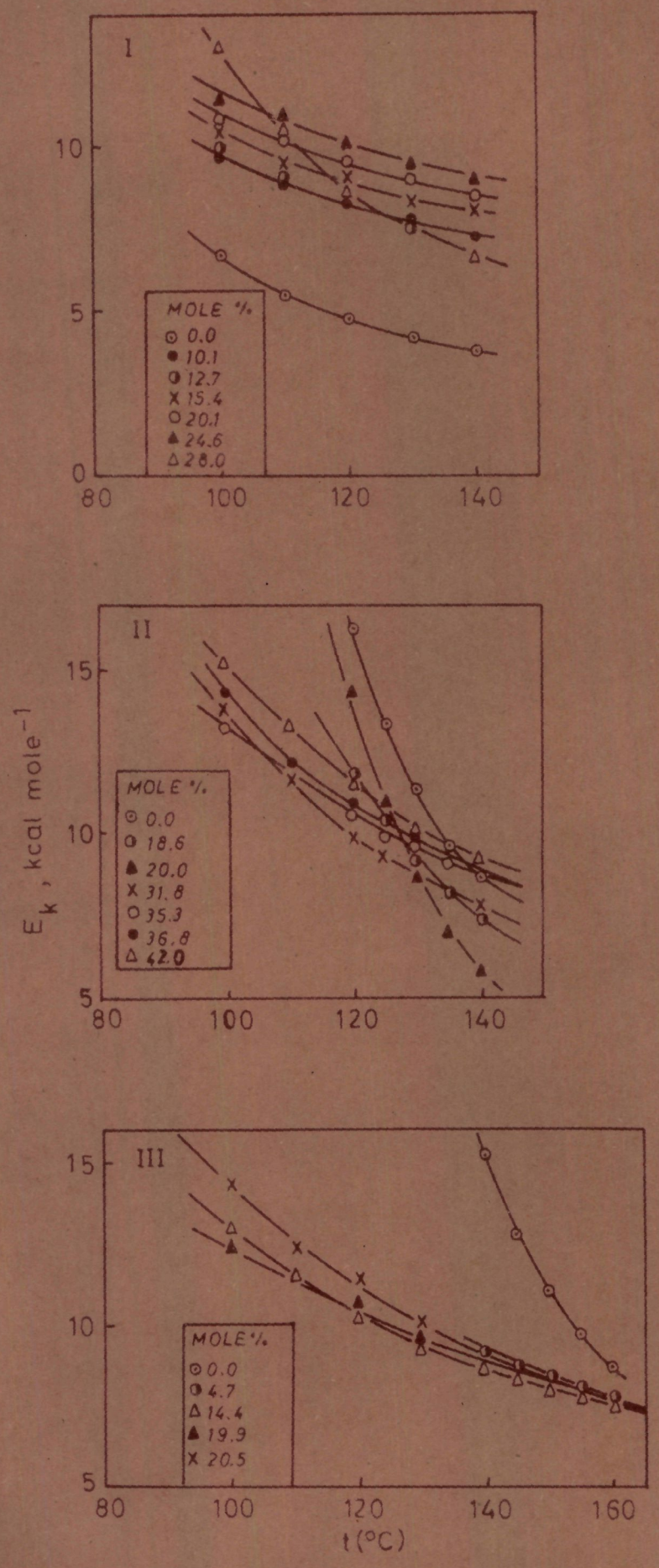

Fig. 2 Energy of activation as a function of temperature for molten salt systems: (I) $MnCl_2$ + Bu_4NCl, (II) $MnCl_2$ + Bu_4NBr, and (III) $MnCl_2$ + Bu_4NI

for the study of electrical conductances of fused salts as temperature independent energy of activation is expected in such an equation. The 'activation energy' obtained from the Arrhenius plots was termed by Angell[1] as 'Arrhenius coefficients' with the restriction that the factor k_Λ should be temperature dependent in the low temperature region. Therefore, it appears reasonable to suppose that such an equation may only find limited applicability in explaining the transport behaviour of such systems. Thus in place of two-parameter equation (rate process theory), three-parameter equations of the type considered in the present discussion appear to be more appropriate and therefore the applicability of the free-volume model may be examined.

The corrected energies of activation, ϵ_{corr} were computed (Table III) using an approximate value of the cubical expansion, α as 1.059×10^{-3} for tetra-n-butylammonium chloride and its mixtures with $SnCl_2$, and 1.0×10^{-3} for the corresponding bromides and iodides. The α for 25 mole % $SnCl_2$ + n-$(C_4H_9)_4NCl$ was calculated at 100°C from the density data described by a linear relation,

$$\rho \ (gm.ml^{-1}) = 1.0209 - 0.9784 \times 10^{-3} \ (t^{\circ}C).$$

The equivalent conductance data were then least square fitted in the equation, $\Lambda = A_\Lambda T^{-\frac{1}{2}} \exp\left[-k_\Lambda/(1-T_0)\right]$ to compute

the T_o values. The computed results of κ_{corr} at several $[T/(T-T_o)]^2$ for the molten salt mixtures have been shown in Fig. 3 in order to examine the validity of the equation:

$$\kappa_{corr} = A\left[\frac{T}{T - T_o}\right]^2 + B$$

It was found in all the cases that these plots (Fig. 3) apparently pass through the origin as expected from the above expression. Slight deviations were observed in the cases of dilute solutions unlike those in concentrated samples. This is an additional support for the use of free volume theory in explaining the electrical conductances of fused salts. The temperature dependence of electrical conductances may prove to be very important in transport processes. This may have direct applications to other processes such as nucleation and growth in amorphous oxide films, where it has been observed that the activation energies are temperature dependent.

The analysis of the specific conductance data show that the exponential dependence of transports on $k'/(T-T_o)$ is a correct formulation. An exponential dependence of transports, expressible as $\exp[-k/R(T-T_o)]$, is based on the free volume model for ionic liquids. The 'free' space or 'free' volume begins to appear above a temperature T_o, consequently below which the free space occurrence vanishes, termed as secondary glass transition temperature, being greater than 0^oK.

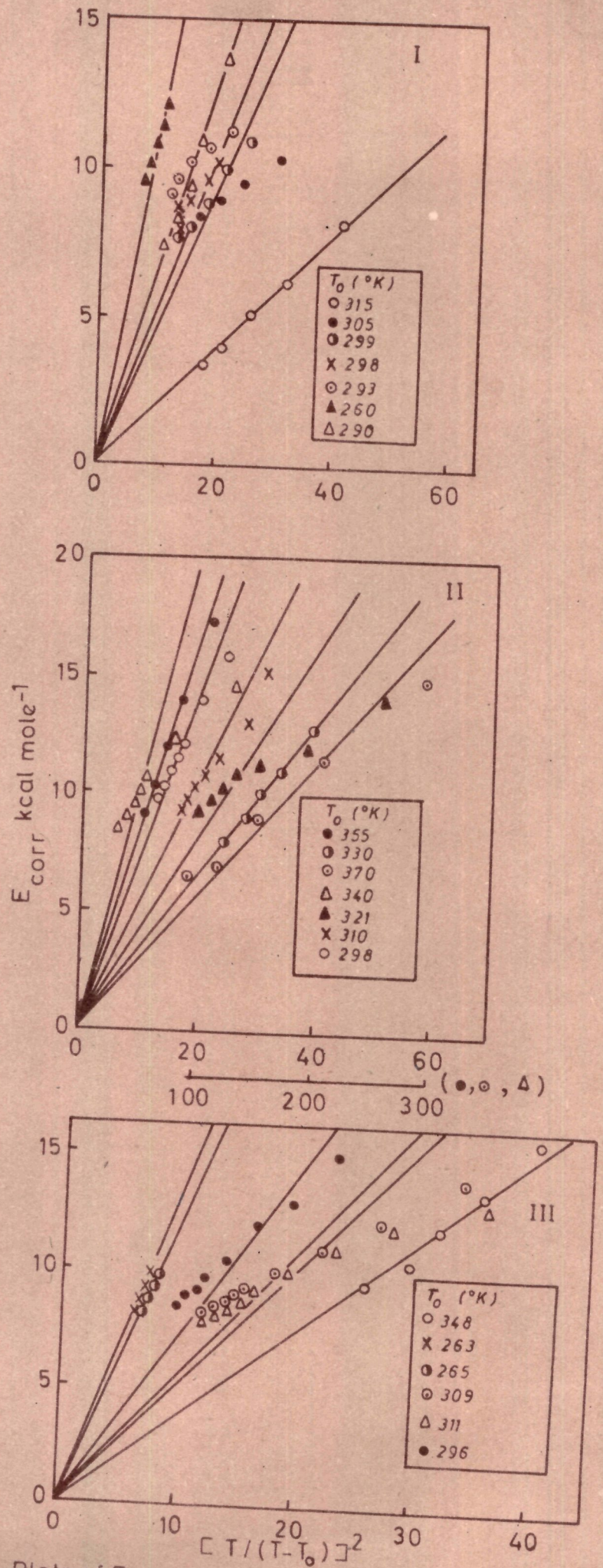

Fig. 3 Plots of E_{corr} vs. $[T/(T-T_o)]^2$ for molten salt systems: (I) $MnCl_2 + Bu_4NCl$, (II) $MnCl_2 + Bu_4NBr$, and (III) $MnCl_2 + Bu_4NI$

Using the values of T_o, plots of log $kT^{\frac{1}{2}}$ vs $1/(T-T_o)$ for the pure n-$(C_4H_9)_4NX$ (X = Cl, Br, I) and those of their mixtures with $MnCl_2$ were made as shown in Fig. 4. These plots may be taken as an equivalent representation of the free volume model. The Arrhenius plots, log k vs. 1/T for dilute solutions are linear[11] whereas such plots are non-linear for the glassy states as apparent from figures 5 and 6. In the case of glassy materials the parameters have been computed using the specific conductances over the entire range of temperature (i.e., above and below the melting points). The log $kT^{\frac{1}{2}}$ values for the glassy materials have been plotted against $1/(T-T_o)$ using the computed value of T_o as shown in Fig. 7. In the case of glassy substances, the T_o values (Table IV) calculated by the best fit method are in good agreement with those obtained by the graphical method[1]. Thus the Arrhenius plots are linear only in the cases of dilute solutions whereas the one based on the free-volume model, i.e. the plots log $kT^{\frac{1}{2}}$ vs $1/(T-T_o)$ are linear for dilute melts as well as for the glassy states. It may be pointed out at this stage that the mechanism of electrical conductance is expected to be independent of the concentration of the melt and therefore the Arrhenius theory of rate processes for the conductances should be replaced by the free volume theory for all the systems under investigation. The E_{corr} and the T_o values for the glassy states have been computed as shown in Table IV. This may further be

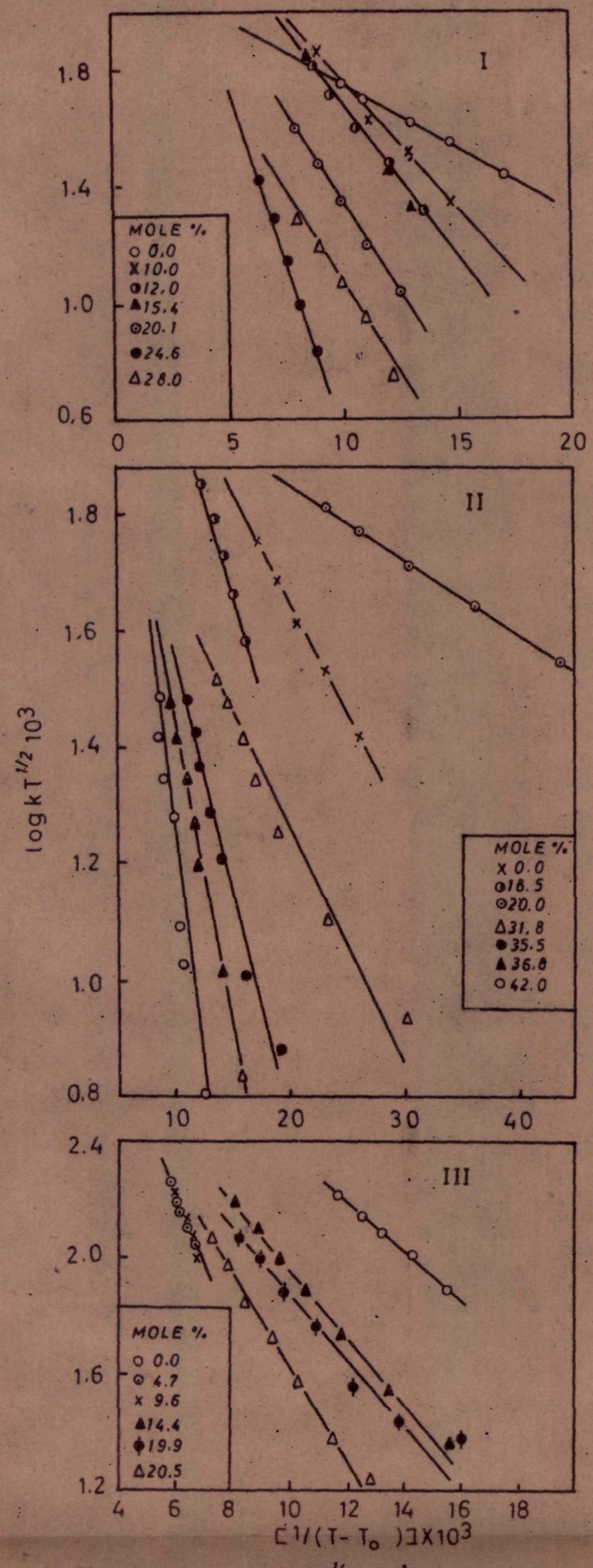

Fig. 4 Plots of $\log kT^{1/2}$ vs. $1/(T-T_o)$ for molten salt systems: (I) $MnCl_2 + Bu_4NCl$, (II) $MnCl_2 + Bu_4NBr$; and (III) $MnCl_2 + Bu_4NI$

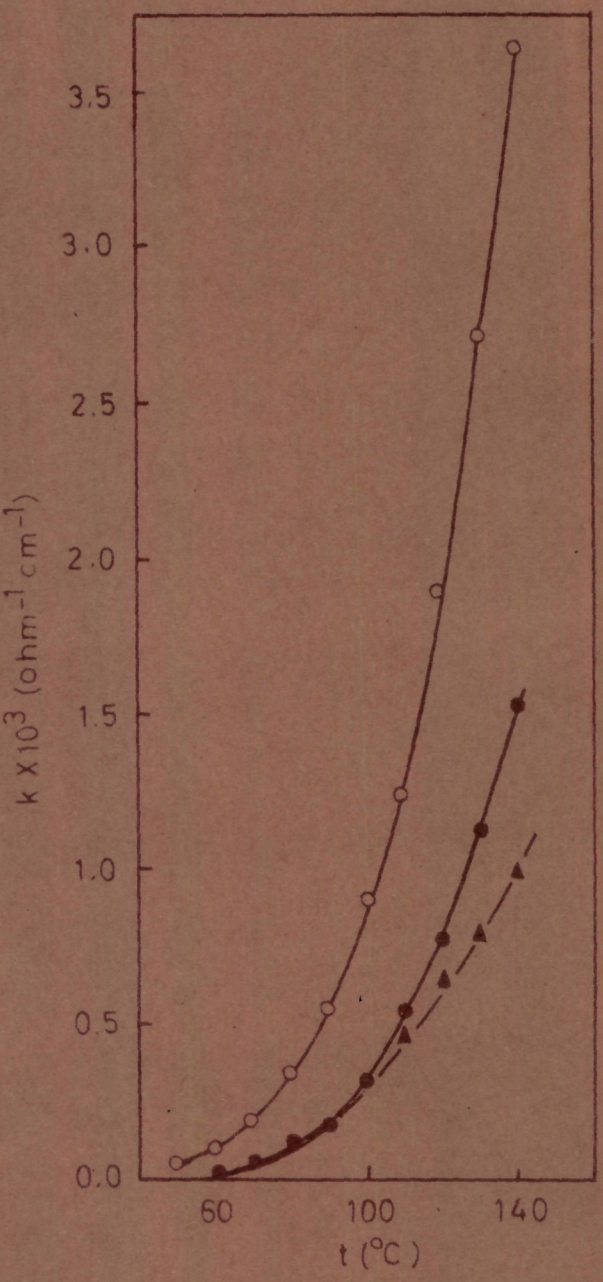

Fig. 5 Specific conductance as a function of temperature for molten salt systems: (▲) $MnCl_2$ (28 mole %) + Bu_4NCl, (●) $MnCl_2$ (42 mole %) + Bu_4NBr, and (o) $MnCl_2$ (20.5 mole %) + Bu_4NI

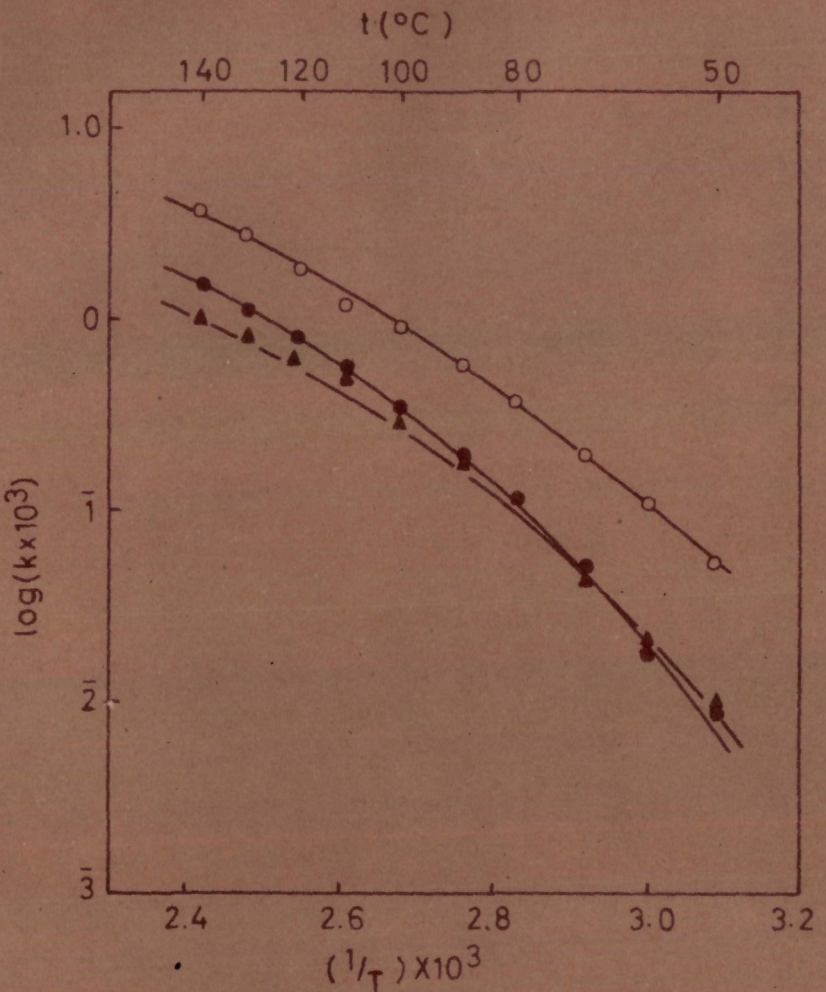

Fig.6 Plots of log k vs. $^1/T$ for molten salt systems: (▲) $MnCl_2$ (28 mole %) + Bu_4NCl, (●) $MnCl_2$ (42 mole %) + Bu_4NBr, and (○) $MnCl_2$ (20.5 mole %) + Bu_4NI

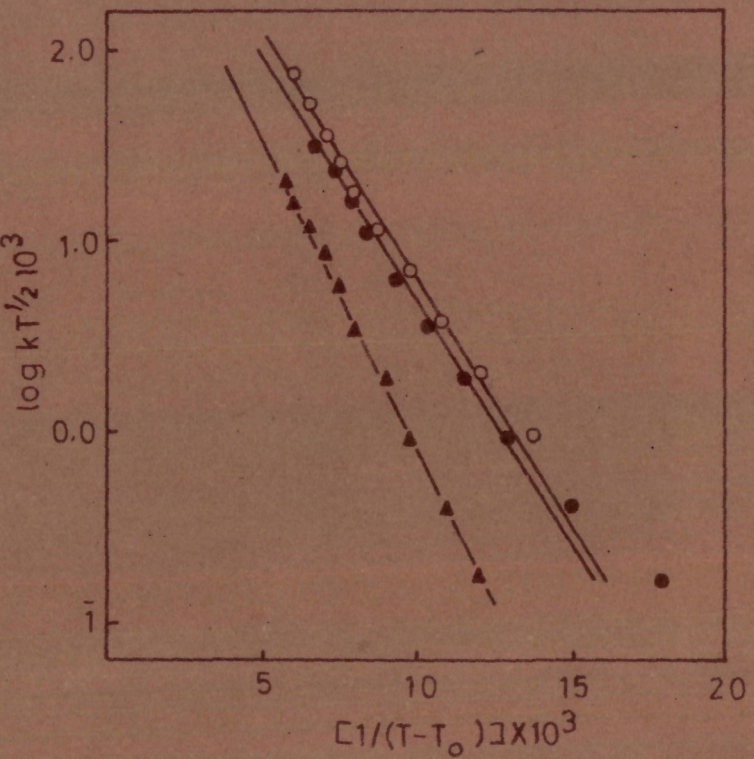

Fig. 7 Plots of log $kT^{1/2}$ vs. $^1/(T-T_o)$ for molten salt systems: (▲) $MnCl_2$ (28 mole %) + Bu_4NCl, (●) $MnCl_2$ (42 mole %) + Bu_4NBr, and (○) $MnCl_2$ (20.5 mole %) + Bu_4NI

TABLE - IV

Computer fitted least square representation of $\Lambda = A_\Lambda^{-1/2} \exp\left[-\frac{k_\Lambda}{T-T_0}\right]$ (323°–413°K) for molten salt systems: $MnCl_2$+Bu_4NX (X=Cl, Br, and I)

Mole %	A_Λ	k_Λ	T_0	Standard Error
28.0 ($X=Cl^-$)	456.91	799.32	240.48	0.005
42.0 ($X=Br^-$)	86.85	483.04	266.88	0.016
20.5 ($X=I^-$)	440.84	569.8	250.09	0.067

verified by the test of results for sensitivity to T_0 of σ_{corr} versus $[T/(T-T_0)]^2$ plots for the three glassy states, 28 mole % $MnCl_2$ in n-$(C_4H_9)_4NCl$, 43 mole % $MnCl_2$ in n-$(C_4H_9)_4NBr$, and 20.5 mole % $MnCl_2$ in n-$(C_4H_9)_4NI$ as shown in Fig. 8. It may, therefore, be generalised that the free volume model explains the behaviour of electrical conductances as is apparent from Figs. 3 and 8 (for several compositions of $MnCl_2$ + n-$(C_4H_9)_4NX$; and the glassy states) as in all the cases these plots pass through the origin.

Physical origin of T_0.

The T_0 values have been found to decrease linearly with composition of $MnCl_2$ in these molten salt mixtures (Table 1), ~~as in other systems[2,4,15]~~. These results are explained in terms of the linear decrease in T_0 values with an increase in the cationic potential.

Since T_0 is dependent on the magnitude of the coulombic binding forces in these systems, the physical origin of the constant may be similar to that suggested by Cohen and Turnbull[14] for molecular liquids. These authors, basing their discussion on Lennard-Jones and Devonshire 6-12 type potential, $V(R)$, for a molecule in a cage formed by near neighbours, suggested that free volume arises when the temperature-dependent average cage

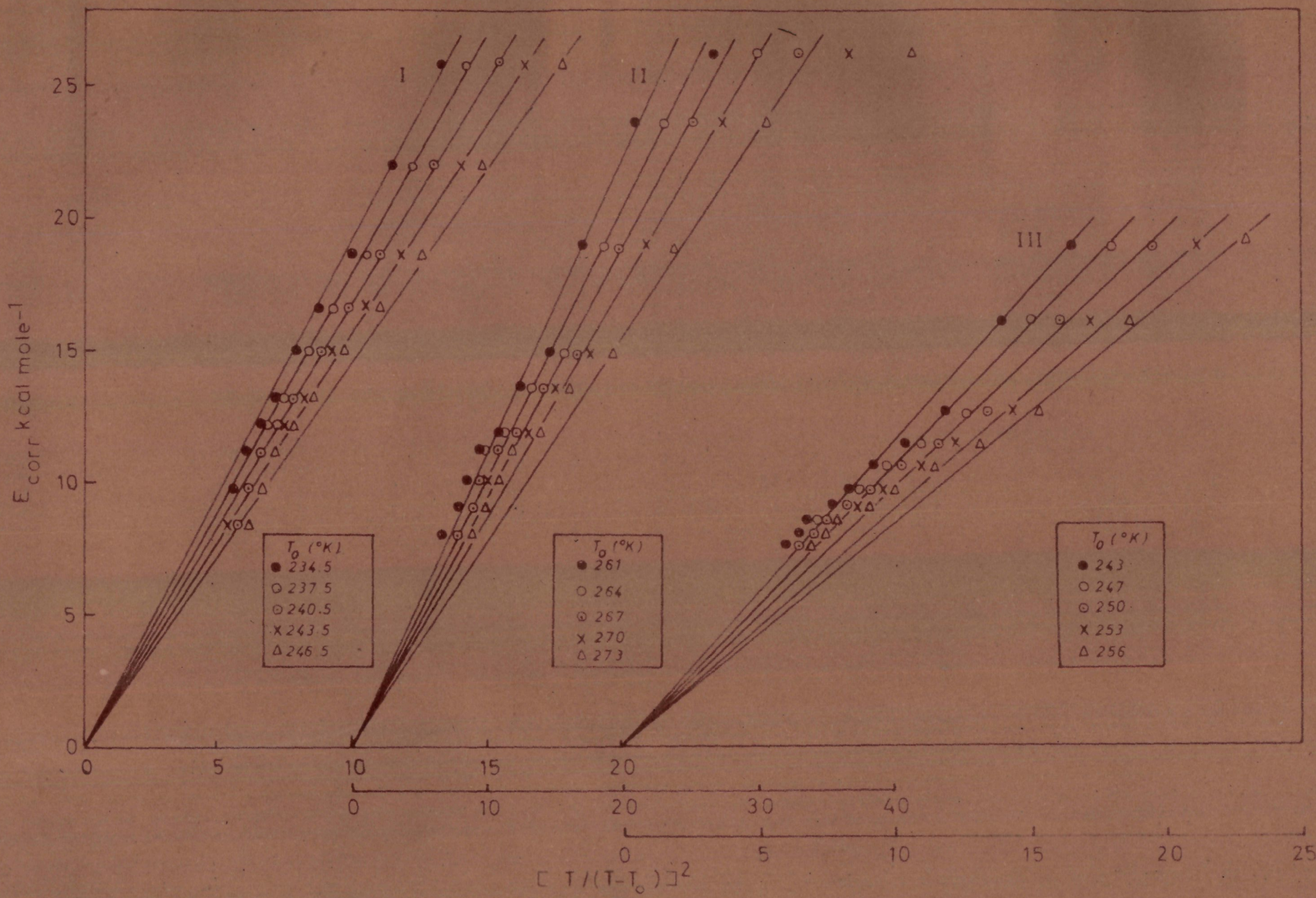

Fig. 8 Test of results of sensitivity to T_o of E_{corr} vs. $[T/(T-T_o)]^2$ plots for molten salt systems: (I) $MnCl_2$ (28 mole %) + Bu_4NCl, (II) $MnCl_2$ (42 mole %) + Bu_4NBr, and (III) $MnCl_2$ (20.5 mole %) + Bu_4NI

radius, R_T, increases to values in the range where $V(R)$ is varying approximately linearly with cage radius R. The fraction of the excess volume, Δv (where Δv=cage volume-molecular volume), appropriate to $R_T - R_{T_o}$, where R_{T_o} is at the edge of the range, was defined as free volume since it would be redistributed among the different cages without over-all energy change, the energy increase of one cage being compensated by a corresponding energy decrease of an adjacent cage. Actually the cage potential in an aggregate can be approximated by a square well potential and T_o should be quite well defined. In the case of an ionic liquid, where the cage particles are of opposite charge compared to the central particle, the cage potential should be an inverse square function of the radius in accordance with the coulomb's law and therefore the single cage potential should be a more gradual function of radius. Kirkwood, et al.[16] have shown, however, that the counter-balancing effects of neighbouring cages would lead to an approximately square well potential for ionic melts. In a stronger force field a higher temperature will obviously be required to realize R_{T_o}. In the light of this viewpoint the physical importance of the systems, $MnCl_2$ + n-$(C_4H_9)_4NX$ (X = Cl, Br and I) may similarly be understood. The $MnCl_2$ -rich mixtures of n-$(C_4H_9)_4NX$ behave as glassy materials as evidenced by their compactness, and transparency at temperatures below the melting points of the parent solvents,

and at the same time behave as ionic liquids at temperatures above the melting points as it is evident from the trend in the behaviour of their measured conductances as a function of temperature. This suggests a compact structure with extremely high viscosity and significantly increased intermolecular forces in the glassy state. This may be explained in terms of cage potential and its dependence on the cage radius which itself is a function of temperature. As the temperature is increased, the compactness is lost due to increased vibrational motion leading to the weakening in the intermolecular forces which leads to the breaking up of the compact structure into simpler species and this may in turn increase the mobility of the ions.

The cause of supercooling may be understood with the help of the free volume model. It may be thought that the complex ions are fewer in the dilute melts, and at the same time the free volumes are densely populated as compared to that in the concentrated solutions, which in turn supports the high value of T_o in dilute solutions and much decreased value in the case of concentrated samples. Therefore, the abundance of free volume and higher T_o values for the dilute melts appear to be responsible for the contraction and a simultaneous cracking and crystallization of such melts on cooling. This process distorts the structural units and causes opaqueness of the cooled molten mixture.

T_o as a basis for corresponding temperatures.

The validity of the equation, $\Lambda = AT^{-\frac{1}{2}} \exp\left[-k_\Lambda/(T-T_o)\right]$ for the systems under discussion has been demonstrated by figures 3 and 8, and also supported by similar plots of log $kT^{\frac{1}{2}}$ vs $1/(T-T_o)$ as shown in figures 4 and 7. Thus T_o may prove a more satisfactory basis for corresponding temperatures in fused salts than the melting point. The usefulness of T_o for this purpose will, of course, depend on establishing the T_o-ionic strength relationship more securely than can be done at the moment.

The constants of the emperical equations.

According to the theory of Cohen and Turnbull[10] developed by Angell[1,17] and others[18], the parameters are composition dependent. The constant k_Λ in the exponential factor of equation $\Lambda = AT^{-\frac{1}{2}} \exp\left[-k_\Lambda/(T-T_o)\right]$ is given by Cohen and Turnbull as

$$k_\Lambda = \frac{\gamma\, v^*}{\alpha\, \bar{v}_m}$$

where v^* is the critical void volume, $\bar{v}_m$ is the mean molecular volume derived from the molar volume, and γ is the factor to correct for overlap of free volume in the calculation of the probability of occurrence of a critical void, and α is the mean expansion coefficient in the range $T-T_o$. The accurate density

data of these systems are not available. However, from the knowledge of the density data of identical systems (to be discussed later) it has been found that the value of α decreases with an increase in the composition of $CoCl_2$ in $n\text{-}(C_4H_9)_4NI$. On this basis it may be thought that the constant k_Λ should be dependent on composition which is in accord with the results presented for the three molten salt systems shown in tables I and IV. Since α varies with composition $\gamma v^*/\bar{v}_m$ itself must be substantially dependent on concentration. It may be suggested that the minimum amount of the solute which will transform the molten solvent into the glassy material on cooling will be guided by the cation-to-anion ratio. The larger the ratio the smaller will be the amount of the solute to be added for the glass formation, the smaller the ratio, the higher the concentrations of the solute required. It may be inferred that besides calculating T_g, and the average disposition of cations about anions, the presence of electrical charges on the conducting species has a considerable effect on their transport behaviour. This is in accord with the conclusions arrived at by Rice[19]. Thus in the present system, $n\text{-}(C_4H_9)_4N^+$ would appear to be less mobile as compared to the halide ion. As $n\text{-}(C_4H_9)_4N^+$ is the larger ion, a high mobility relative to that of halide ion would conflict with both Rice's view that only short range forces should decide relative transport rates in fused salts[19], and

with the complementary expectation that free volume alone determines the transport rates. Thus the addition of $MnCl_2$ may be considered as the process of packing the empty sites with the salt in the molten solvent which eventually leaves only few unbound or free solvent anions. This sort of packing, after a certain critical stage becomes so tight and compact that any further addition becomes impossible. Moreover, the time taken in this process of concentration build up increases from four hours to more than a week. This increasingly slow process is the result of compact packing which takes time in forcing the extra added solute to enable it to creep into the empty sites for the occupancy. Such a tight packing may prevent any positional disorder on cooling the concentrated mixture. Therefore the chilled mixture stays as transparent glassy material which in turn freezes the mobility of the ions.

The pre-exponential constant.

The pre-exponential constant suggested by Cohen and Turnbull implies a direct dependence on particle diameter and an inverse dependence on the square root of the particle mass. In fused salts the jump distance would have to include the diameters of both cations and anions since an ion must cross the first coordination shell of oppositely charged ions to reach

its new equilibrium position. Hence the pre-exponential constants for cations and anions in a pure fused salt should be insensitive to the particle radii and depend only on the relative ionic masses.

Calculations of A_λ's for the systems considered in this discussion are given in tables I and IV for molten $MnCl_2$ + n-$(C_4H_9)_4NX$ (X = Cl, Br and I) and their glassy states respectively. It is seen that the pre-exponential constants are incorrectly dependent on composition.

ELECTRICAL CONDUCTANCE AND THE GLASS-FORMING TENDENCY OF MOLTEN SALT MIXTURES OF COBALT(II) CHLORIDE AND TETRA-n-BUTYLAMMONIUM IODIDE

Experimental

Chemicals.

Tetra-n-butylammonium iodide (Eastman, Kodak) was recrystallised several times from acetone-ether mixture[20]. Acetone and ether (AR, BDH) were purified[21] by successive distillation. Anhydrous $CeCl_3$ was prepared from its recrystallised hydrated salt. Quinoline (BDH) and commercial linseed oil were used for the purification of thionyl chloride. Purified and distilled thionyl chloride (Riedel) was used as a dehydrating agent for the preparation of $CeCl_3$. Potassium chloride (AR, BDH) was used for the calibration of the conductivity cell.

Recrystallisation of $n\text{-}(C_4H_9)_4NI$[20].

Tetra-n-butylammonium iodide was dissolved in a mixture of acetone and ether. Great care was taken to ensure that the ether was peroxide free and the acetone was redistilled. The salt was dissolved in a minimum amount of acetone, and ether was added until precipitation commenced, at which point the solution cooled and the resulting crystals were filtered in a fritted glass funnel. After a preliminary drying, the salts

were finely ground and dried in vacuum over P_2O_5 at 80°C.

Purification of acetone[21].

Acetone was refluxed with successive small quantities of potassium permanganate until the violet colour persisted. It was then dried with anhydrous potassium carbonate or anhydrous calcium sulphate, filtered from the desiccant and fractionated. Precautions were taken to exclude moisture.

Purification of ether[21].

In order to remove the peroxides, ether was washed with concentrated solution of ferrous sulphate and triply distilled water and separated. It was dried over anhydrous calcium chloride and then distilled. The distilled ether was transferred to a coloured bottle, and then sodium wire was introduced directly into the ether and was allowed to stand for 24 hours for removing even the last traces of moisture.

Purification of thionyl chloride[21].

The commercial thionyl chloride was first fractionated in all glass apparatus from quinoline in order to remove acid impurities. The distillate was then refractionated as before from boiled linseed oil. The fraction was collected in a well

fitted glass stoppered bottle.

Preparation of anhydrous cobalt(II) chloride[32].

The hydrated salt was treated with freshly distilled thionyl chloride until all the sulphur dioxide was completely removed. The excess of thionyl chloride was removed by distillation in vacuo using a pure dry nitrogen bleed. The final product was finely ground and was stored in a vacuum desiccator over potassium hydroxide.

Instrumentation.

The conductance measurements were made with a conductivity bridge of Philips Type-PW9509 at a frequency of 50 c/s. The dielectric constant of the molten sample, 31.5 mole % $CoCl_2$ in n-$(C_4H_9)_4NI$ was measured with the Sargent Chemical Cecilometer-Model No. V.

A number of conductivity cells of capillary type of different dimensions were made of pyrex glass. The platinum electrodes and a thermometer were placed in the U-tube of the cell. The cell was calibrated with 0.1F KCl solution at 25°C. The cell was immersed in a thermostated oil bath (same as described earlier) which was placed in a dry box.

Procedure.

A weighed amount of the recrystallised tetra-n-butyl-ammonium iodide was taken in a boiling tube and placed in the jacket of the thermostated oil bath. A weighed amount of anhydrous cobaltous chloride was added to the molten solvent and the mixture was heated until a clear solution was obtained. The dilute solutions required approximately 6-8 hours of heating for obtaining clear solution while concentrated solutions required a few days. The sample was transferred to the conductivity cell and its conductances were measured at several temperatures. Similarly a number of solutions of different compositions were prepared and their conductances measured.

The cell constant determined at 25°C for different cells are given in Table V. The conductance of pure molten n-$(C_4H_9)_4NBr$ was measured as functions of temperature and frequency and the results agree within $(\pm 0.1)10^{-3}$ ohm^{-1}.

A capillary-type conductivity cell (cell constant 1612 cm^{-1}) was used for the conductance measurements. The conductances of these mixtures were measured at an interval of 10° over a range of 373°-413°K with an accuracy of $\pm$ 0.03 ohm^{-1}. The conductivity cell was cleaned with hot distilled water and soaked overnight in conductivity water and the cell constant was checked after each set of measurement.

The density measurements were made in a pyknometer. The pyknometer was calibrated before use with purified quinoline of known densities[23]. The samples were transferred to the pyknometer with the help of a vacuum pump and the changes in volume were recorded as a function of temperature. The correction for cubical expansion was compensated in calibration. The preparation of the samples and the measurements were carried out in a dry box.

RESULTS AND DISCUSSION

The resistances of pure n-$(C_4H_9)_4NBr$ were measured in several cells as a function of frequency. The specific conductances obtained with different cells at different frequencies (i.e., 50 and 1000 c/s) are given in Table V. It appears from the table that the high value of cell constants has very little effect on the measured resistances of low melting salts. For a given frequency, the specific conductance has been found to be almost independent of the cell constant (1401 cm^{-1}, 1140.3 cm^{-1}, 641.1 cm^{-1} and 25 cm^{-1}). The effect of frequency on specific conductance, k is also not very significant.

A calibration curve for the instrument response versus dielectric constant ϵ was made using water, quinoline, methanol, benzene, acetone, chloroform, ethanol, acetyl chloride and nitrobenzene as standard liquids, and the dielectric constant of the glassy material (31.5 mole % $CoCl_2$ in n-$(C_4H_9)_4NI$) was obtained from such a curve by interpolation. The capacitance of the electrical double layer of the molten salt mixture was calculated (Appendix E). It was found that the measured capacitance C' for the cell used was of the order of (3-6) x 10^{-4} picofarads. The corresponding magnitude of impedence (ac analog of resistance, i.e., ratio of voltage to current), $1/2\pi fC'$,

TABLE - V

Specific conductance as functions of cell constant and frequency for pure molten Bu_4NBr

Temp. (°C)	Cell constant= 1401.0 cm^{-1}		Cell constant= 1140.3 cm^{-1}		Cell constant= 641.1 cm^{-1}		Cell constant = 28.0 cm^{-1}	
	Frequency		Frequency		Frequency		Frequency	
	50 c/s k x 10^3	1 k c/s k x 10^3	50 c/s k x 10^3	1 k c/s k x 10^3	50 c/s k x 10^3	1 k c/s k x 10^3	50 c/s k x 10^3	1 k c/s k x 10^3
121	1.384	1.997	1.461	1.923	1.503	1.817	1.728	1.817
124	1.484	2.488	1.536	2.578	1.675	2.147	2.099	2.147
127	1.667	2.838	1.755	2.900	1.803	2.378	2.214	2.378
130	1.972	3.017	1.899	3.135	1.915	2.624	2.554	2.624
133	2.005	3.545	2.068	3.453	2.095	2.909	2.834	2.909
136	2.132	4.062	2.202	3.696	2.311	3.334	3.149	3.334

is of the order of (0.5-1) x 10^{13} ohm at 50 c/s in parallel with the electrolyte resistance, and therefore, has little effect on the measured resistances.

According to Braunstein[24], the magnitude of the double layer capacitance for electrolyte-electrode systems in molten salts is of the order 10-100 microfarads per cm^2 of electrode surface. This leads to a magnitude of impedence at 50 c/s of the order

$$\frac{1}{2\pi fC} = \frac{1}{6.28C} \approx 31.8 - 318 \text{ ohm}$$

at a 1 cm^2 electrode. Thus the high value of impedence in series shows that the capacitance is very small and hence both the parallel and double-layer capacitance factors will not affect the measured resistances. Therefore, the capacitive factor was not taken into consideration in these measurements.

The resistances of molten mixtures of $CoCl_2$ and n-$(C_4H_9)_4NI$ were measured as functions of temperature and composition. These measurements were made in a cell whose cell constant was 1612 cm^{-1} at a frequency of 50 c/s. The temperature range of measurement was 373°-413°K. The specific conductances of molten mixtures of $CoCl_2$ and n-$(C_4H_9)_4NI$ are temperature dependent and have been plotted as log k vs 1/T (Fig. 9). The plots of log k vs 1/T are curvilinear. The transport behaviour of such ionic liquids are similar to those described earlier. It may therefore be assumed

that the entire conductance data of these systems might follow the pattern reported recently by Angell[1,17,25,26] and Moynihan[27,28]. Therefore, the specific conductance data of molten mixtures of $CoCl_2$ and $n\text{-}(C_4H_9)_4NI$ have been examined in the light of the theory proposed by Cohen and Turnbull[10,14]. Although the range of temperature measurement is low, the consistent pattern of transport behaviour of this system like those of earlier results need to be analysed in the light of different emperical equations based on free volume model for ionic liquids.

The equivalent conductances were calculated with the help of the density data (Table VI) and were least square fitted to the equation,

$$\Lambda = AT^{-\frac{1}{2}} \exp\left[-k_\Lambda/(T-T_0)\right] \text{ - - - - - - - (1)}$$

Since the plots of log k vs 1/T (Fig. 9) are non-linear as in the case of $MnCl_2$ + Bu_4NX systems, the plots of $\log \Lambda T^{\frac{1}{2}}$ vs $1/(T-T_0)$ should be linear for the appropriate choice of T_0 (Fig. 10). It is seen that the linear plots support the correlation of T_0 based on the free volume model. The presence of $T^{\frac{1}{2}}$ in the pre-exponential term of the above equation has been taken into account in these plots. However, the term $T^{\frac{1}{2}}$ has a little influence on the linearity of the $1/(T-T_0)$ plots in the low temperature region and hence has been included in figure 10 in order to examine the applicability of the equation

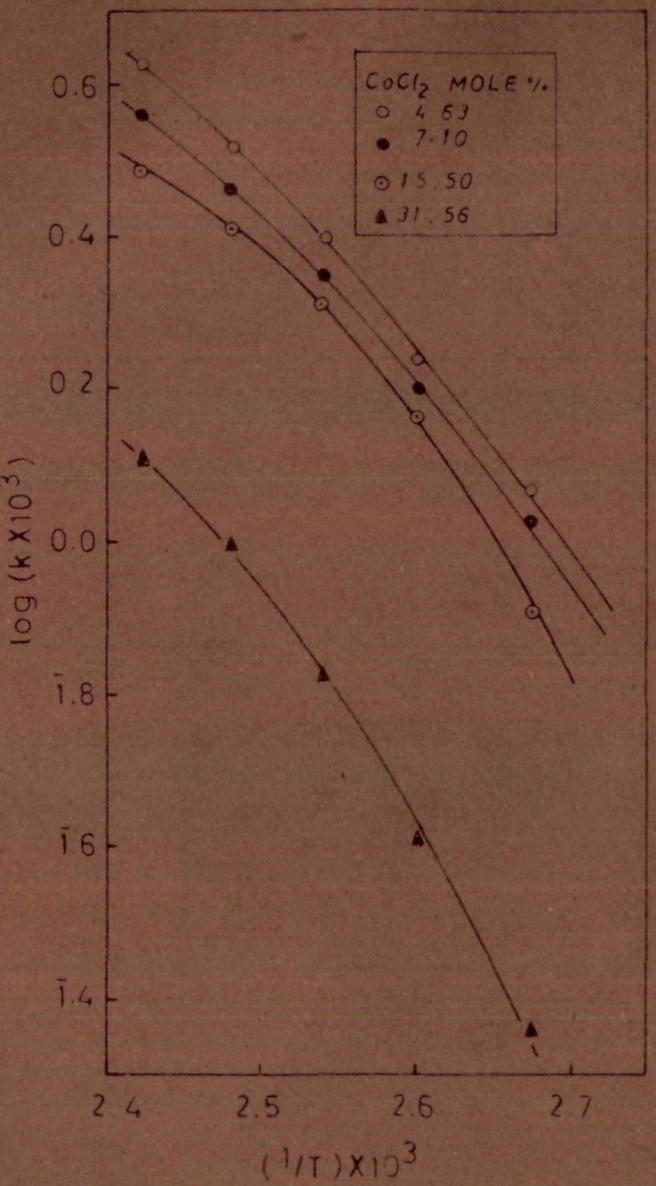

Fig 9 Plots of log k vs 1/T for molten mixtures of $CoCl_2$ and Bu_4NI

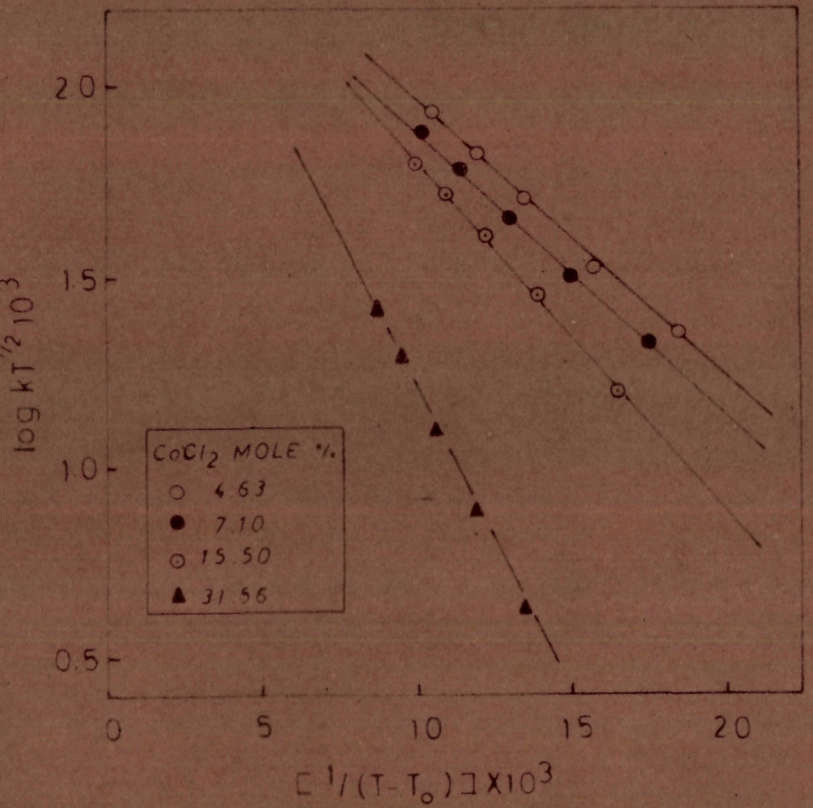

Fig 10 Plots of log $kT^{1/2}$ vs $1/(T-T_o)$ for molten mixtures of $CoCl_2$ and Bu_4NI

TABLE - VI

Density and coefficient of expansion as a function of temperature for molten mixtures of $CoCl_2$ and Bu_4NI.

t(°C)	4.6 mole %	7.1 mole %	15.5 mole %	31.5 mole %
	$\rho(gm\ ml^{-1})=$ 1.2287-0.6999 x $10^{-3}(t)$	$\rho(gm\ ml^{-1})=$ 1.2596-0.7265 x $10^{-3}(t)$	$\rho(gm\ ml^{-1})=$ 1.2848-0.713 x $10^{-3}(t)$	$\rho(gm\ ml^{-1})=$ 1.3206-0.7021 x$10^{-3}(t)$
	α x 10^4	α x 10^4	α x 10^4	α x 10^4
100	6.040	6.120	5.878	5.614
105	6.059	6.139	5.893	5.629
110	6.077	6.158	5.910	5.645
115	6.095	6.177	5.928	5.661
120	6.114	6.196	5.946	5.678
125	6.133	6.215	5.963	5.693
130	6.152	6.234	5.981	5.710
135	6.172	6.254	6.000	5.726
140	6.189	6.274	6.017	5.743

(1). In this figure the linear temperature plots justify the appropriate choice of T_o. The values of E_Λ are independent of temperature as evidenced by the foregoing discussion. The best choices of T_o are made by the best fit to equation (1) of the equivalent conductance data by minimising the standard error between the experimental and the calculated values (Table VII).

The specific conductance data of molten mixtures of $CoCl_2$ and $n\text{-}(C_4H_9)_4NI$ were least square fitted in different functional forms as shown in Table VII. The parameters are temperature independent and composition dependent as has been found in earlier results. The energies of activation for specific conductance, E_κ's were computed over a specified range of temperature from the derivatives[18] of two analytical expressions for specific conductance as shown in Appendix B. The energy of activation for specific conductance, E_κ was also calculated from the successive pairs of points (average 3° interval) from the plot of log κ vs $1/T$. The energies of activation, E_κ's obtained by different methods were averaged (Table VIII) and plotted as a function of composition (Fig. 11). The energy of activation for equivalent conductance, E_Λ was calculated from the derivative $\left[-d\ln\Lambda/d(T^{-1})\right]$ (Appendix B) and plotted as a function of temperature (Fig. 12). Using the average values of E_κ's, the corrected values of activation energy, E_{corr} were calculated over specified range of temperature (Table VIII).

TABLE - VII

Computer fitted least square representation for specific and equivalent conductances as a function of temperature* (373° - 413°K) for molten mixtures of $CeCl_3$ and Bu_4NI

Mole % $CeCl_3$	Equation No.	a	b	c	Standard Error
	(i)	0.2707×10^{-2}	-0.8100×10^{-4}	0.6532×10^{-6}	0.04
4.63	(ii)	0.0829	391.6	282.2	0.04
	(iii)	149.4	168.3	320.1	0.04
	(i)	-0.0918×10^{-2}	-0.1254×10^{-4}	0.3204×10^{-6}	0.02
7.1	(ii)	0.0319	238.7	303.6	0.02
	(iii)	127.8	214.2	316.8	0.02
	(i)	-0.001×10^{-2}	-0.2472×10^{-4}	0.3382×10^{-6}	0.1
15.5	(ii)	0.0228	205.2	309.9	0.1
	(iii)	137.5	216.1	313.1	0.02
	(i)	0.10867×10^{-2}	-0.3506×10^{-4}	0.2622×10^{-6}	0.02
31.5	(ii)	0.0158	229.96	320.62	0.02
	(iii)	154.02	391.3	299.7	0.003

(* t°C, T°K) (i) $k=a+bt+ct^2$; (ii) $k=a \exp\left[\frac{-b}{T-c}\right]$ and (iii) $\Lambda=aT^{-\frac{1}{2}} \exp\left[\frac{-b}{T-c}\right]$

TABLE - VIII

Computed results of activation energy, E_{corr} as a function of temperature for molten mixtures of $CoCl_2$ and Bu_4NI.

	4.6 mole %					7.1 mole %				
T(°K)	$\propto RT^2+\frac{1}{2}RT$ (kcal/mole)	E_k^1	E_k^2 (kcal/mole*)	E_k^3	E_{corr} (kcal/mole)	$\propto RT^2+\frac{1}{2}RT$ (kcal/mole)	E_k^1	E_k^2 (kcal/mole*)	E_k^3	E_{corr} (kcal/mole)
373	0.538	12.05	13.14	13.71	13.69	0.540	13.81	13.72	13.71	14.32
378	0.548	11.36	12.12	12.15	12.49	0.550	11.98	12.26	12.16	12.68
383	0.558	10.75	11.24	11.42	11.27	0.560	10.69	11.05	11.43	11.62
388	0.568	10.20	10.47	10.26	10.88	0.570	9.74	10.00	10.65	10.70
393	0.578	9.72	9.79	9.82	10.35	0.581	9.02	9.18	9.14	9.69
398	0.588	9.29	9.19	9.14	9.75	0.591	8.44	8.44	8.27	8.97
403	0.599	8.91	8.66	8.23	9.10	0.601	7.97	7.81	7.45	8.14
408	0.609	8.58	8.19	7.71	8.61	0.612	7.58	7.25	6.85	7.84
413	0.620	8.28	7.76	6.95	8.15	0.623	7.25	6.78	6.08	7.32

* E_k^1, from the derivative of $a+bt+ct^2$; E_k^2, from the derivative of $a\exp[-b/(T-c)]$ and E_k^3, from the slope of Arrhenius plot, log k vs. 1/T.

TABLE - VIII(Contd.)

T(°K)	15.5 mole %					31.5 mole %				
	$\alpha RT^2+\frac{1}{2}RT$ (kcal/mole)	ε_k^1	ε_k^2 (kcal/mole*)	ε_k^3	ε_{corr} (kcal/mole)	$\alpha RT^2+\frac{1}{2}RT$ (kcal/mole)	ε_k^1	ε_k^2 (kcal/mole*)	ε_k^3	ε_{corr} (kcal/mole)
373	0.533	13.13	14.25	13.71	14.22	0.528	23.73	23.17	23.99	24.16
378	0.543	11.63	12.56	12.79	12.66	0.535	19.20	19.83	18.28	19.64
383	0.553	10.60	11.19	11.42	11.62	0.545	16.39	17.22	17.14	17.47
388	0.563	9.78	10.06	10.28	10.60	0.555	14.47	15.15	15.22	15.51
393	0.573	9.13	9.12	9.14	9.70	0.565	13.06	13.47	13.71	13.98
398	0.583	8.39	8.61	8.32	8.97	0.575	11.99	12.09	12.79	12.84
403	0.593	8.17	7.64	7.76	8.46	0.585	11.13	10.94	11.42	11.75
408	0.603	7.81	7.05	7.31	7.99	0.595	10.44	9.96	10.28	10.83
413	0.614	7.50	6.54	6.85	7.57	0.606	9.87	9.13	9.14	9.99

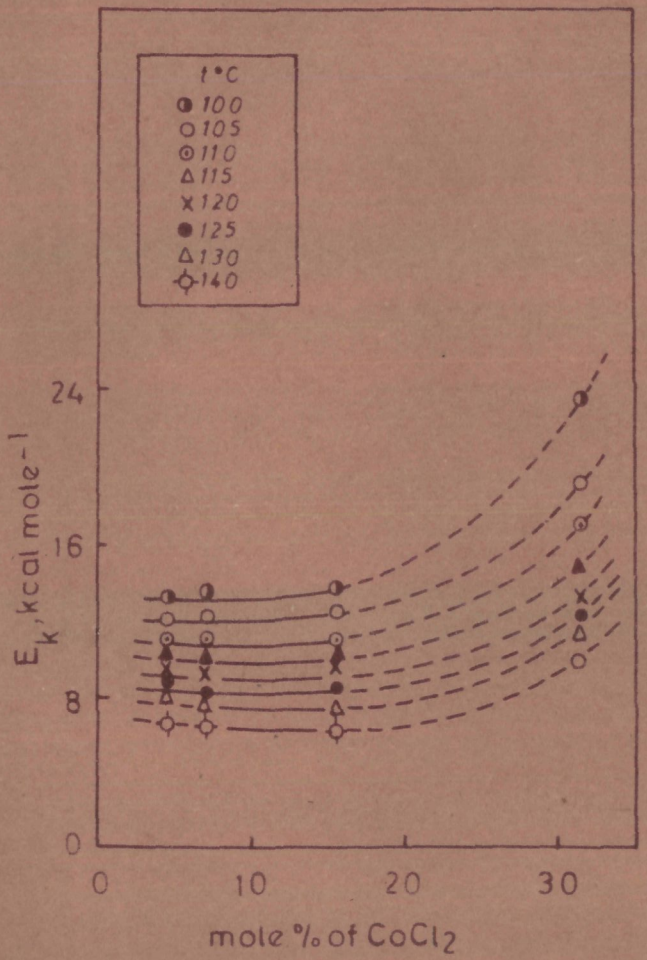

Fig. 11 Energy of activation as a function of composition for molten mixtures of $CoCl_2$ and Bu_4NI

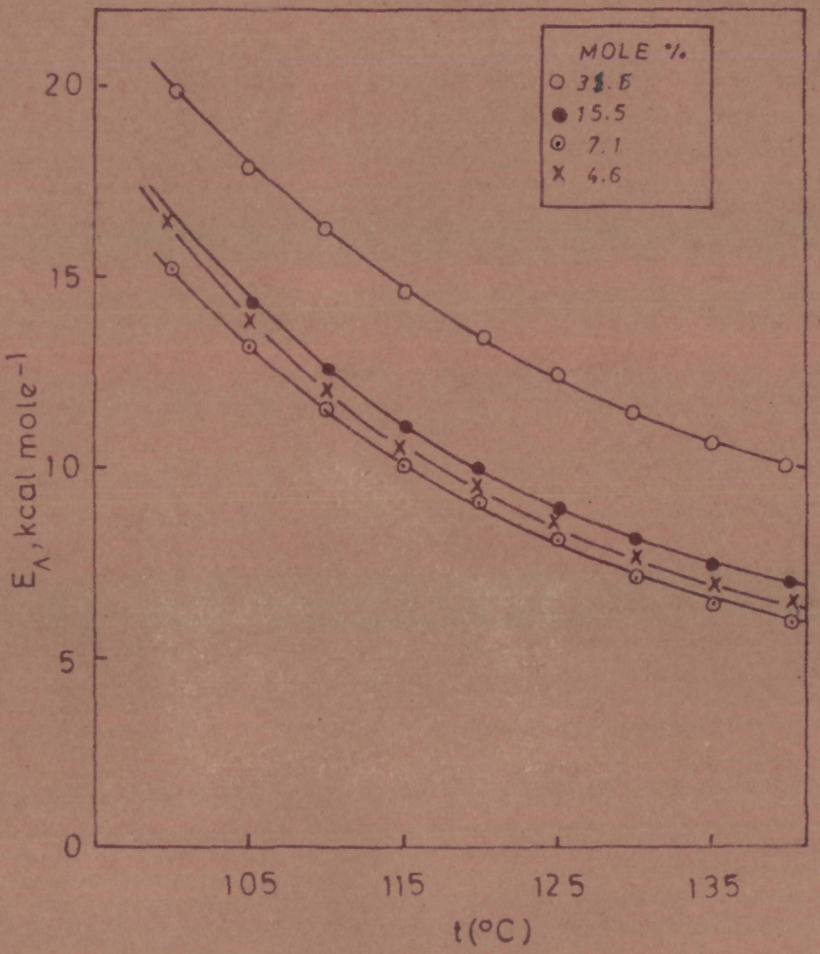

Fig. 12 Energy of activation as a function of temperature for molten mixtures of $CoCl_2$ and Bu_4NI

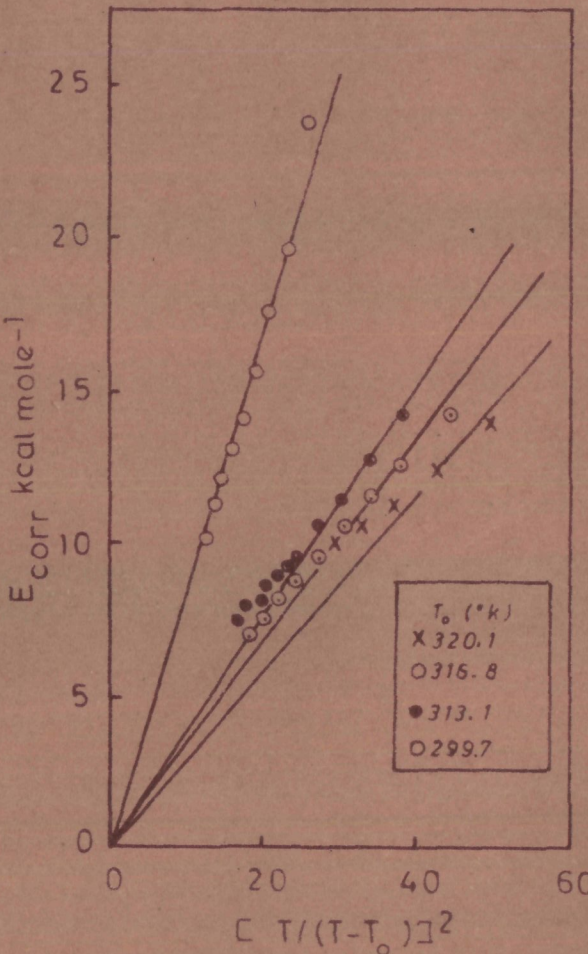

Fig. 13 Plots of E_{corr} vs. $[T/(T-T_o)]^2$ for molten mixtures of $CoCl_2$ and Bu_4N

The coefficient of expansion, α at different temperatures were calculated from their density data as given in Table VI. The computed results of E_{corr} for several compositions of $CoCl_2$ in $n\text{-}(C_4H_9)_4NI$ were plotted as a function of $[T/(T-T_0)]^2$ as shown in figure 13.

It is clear from figures 11 and 12 that the energy of activation is linearly dependent on temperature and the change in activation energy is large enough in the low temperature region. However, the activation energy increases with an increase in mole % of $CoCl_2$ (Fig. 11) which may be due to the complex formation as evidenced by the spectral studies of the glassy material and its comparison with those of similar systems[4,12]. The plots of E_{corr} vs $[T/(T-T_0)]^2$ have been found to pass through the origin (Fig. 13). However, more deviation was found in the case of dilute solutions specially at higher temperatures. In the case of dilute solutions the deviation is not surprising, as accurate values of T_0 cannot be determined due to crystallisation[10]. However, it appears from figures 11-13 that the results are in accordance with the free volume model and also account for the nucleation (as E_g varies with T) which leads to the formation of glassy materials as described earlier.

It may be recognized that the plots of log k vs 1/T are curvilinear which become linear by the introduction of a third

adjustable parameter, T_0 (Fig. 10). The parameter T_0 has been found to be linearly related to composition and it may have the expected relation to the glass transition temperature[1,17]. Thus in support of this view, the relationship between T_0 values and the cationic strength of $CoCl_2$ has been shown in Fig. 14. It has been found that the T_0 values decrease linearly with the increase in cationic potential (i.e. $\sum_i N_i Z_i / r_i$ where N_i is the mole fraction of i th ion, Z_i = ionic charge, and r_i = ionic radii[39]) and support the concept of free volume model for ionic liquids.

The spectral studies reinforces our conclusion regarding the complex formation in these media. As the amount of $CoCl_2$ is increased, the more mobile anions (relative to $n\text{-}(C_4H_9)_4N^+$ ion) get tied up to the metal ion, constituting a compact, and ordered structure, whereby decreasing the overall free volume. This view is supported by the low value of conductance with an increase in the composition of $CoCl_2$. Thus the process of adding $CoCl_2$ may be taken as the way of packing the free space available in the mixtures. A state arises, when further addition of $CoCl_2$ becomes impossible and the mixture does not crystallize on cooling. Thus the complex formation lowers the T_0 values presumably indicating the absence of free volume below that temperature. It may be expected that in the absence of crystallization, addition of an excess amount of a solute to

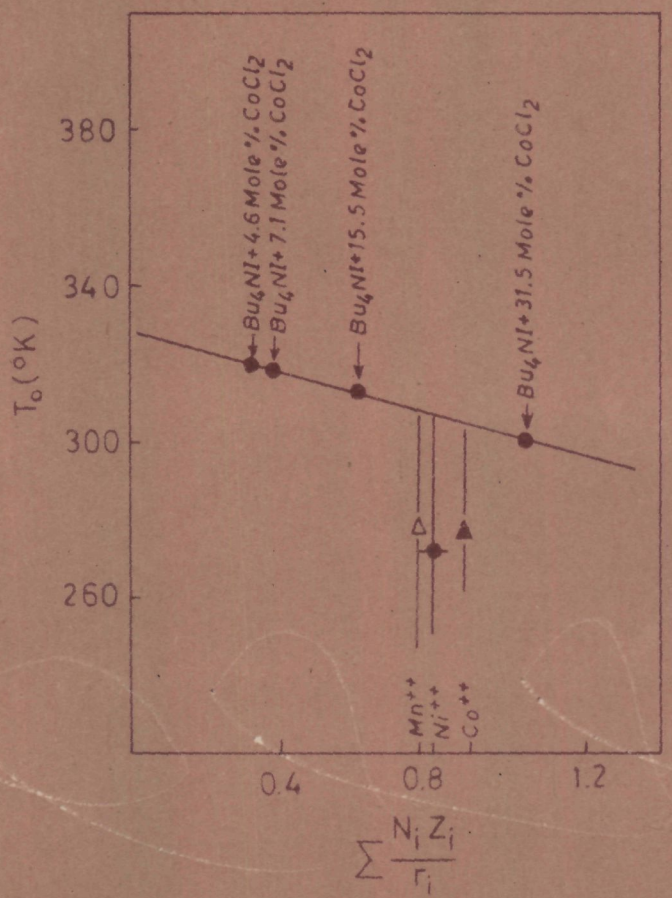

Fig 14 Relationship between T_o and cationic strength of various molten salt mixtures

any ionic solution results in glass formation. It must be noted that solutions of most uni-univalent salts could never be obtained as glassy material by increasing the concentration of the solute in the molten ionic liquid and then cooling it to the room temperature, because the glass transition temperature for the pure metastable liquid salt itself will be below room temperature, e.g. for KNO_3, $T_g \approx 230^{\circ}K$[1]. Owing to this paramount importance in this discussion, however, we wish to emphasize at this point that the familiar salt of multivalent cations exhibit a physically meaningful concentration for a given temperature at which the 'solution' would lose its liquid character and form a glass. This concentration which will be designated as N_g, will be seen subsequently to play an important role in the interpretation of the isothermal composition dependence of the transport properties analogous to that of T_g in the earlier interpretation of the temperature dependence of conductance for the systems under discussion. This is based on the validity of the equation (1) for the temperature dependence of conductance. It is therefore interesting to examine the importance of this equation in the molten salt systems.

Concentration dependence of conductance.

The Arrhenius coefficient $\left[-R d\ln \Lambda / d(T^{-1})\right]$ for several compositions may be evaluated in order to study the behaviour of

T_o with composition. As the Arrhenius plots (Fig. 9) are curvilinear, Arrhenius coefficients for both specific and equivalent conductances are temperature dependent as has been shown in figure 12. From the present data and those of Moynihan[28] who has studied both viscosity and conductance, it appears that equation (1) gives a correct formulation of the dependence of transport on temperature for molten salt systems. In view of its validity for other liquids[30-32] it seems safe to assume its continuing validity for less concentrated solutions. Furthermore the constant k_Λ seems to be insensitive to the nature of the liquid being described earlier[25]. But in the case of molten salt systems under discussion the constant k_Λ is sensitive towards the nature of the liquid as apparent from Table VIII where these data have been computed from the best fit of equation (1). It therefore, appears that significant changes in transport properties as a function of composition should be attributed mainly to changes in T_o. The magnitude of T_o for liquids composed of simple particles is evidently some reflection of the cohesive energy of the liquid. This is implied by the correlation of T_o with the cationic potential (Fig. 14). In the case of solution of nonassociating charged particles in a molecular solvent, the coulombic energy may be determined by the physical concentration of electrostatic charge so a correlation between T_o and conventional concentration, N, of the solution might be anticipated.

The concentration N may be expressed as mole fraction. Let us suppose that K_Λ and A_Λ of equation (1) are composition invariant and Γ_o is linearly dependent on the charge concentration, N. Then for a given concentration, N, Γ_o of equation (1) is given by

$$\Gamma_{o(N)} = QN + \Gamma_{o(N=o)}$$

where $\Gamma_{o(N=o)}$ is the value of Γ_o at infinite dilution, i.e., Γ_o for the solvent. Recalling the initial discussion it is possible in principle to specify a limiting concentration, N_o, for which the value of Γ_o becomes equal to the isothermal temperature T and the ionic mobility falls to zero. Using equation (2), T of equation (1) can therefore be replaced by

$$\left[QN_{o(T)} + \Gamma_{o(N=o)}\right]$$

Making these substitutions for Γ_o and T in equation (1) one can obtain the following expression for the isothermal conductance.

$$\Lambda = A'_\Lambda \exp\left[-(B_\Lambda/Q)/(N_o-N)\right] - - - - - - - (3)$$

It is to be noted that $\Gamma_{o(N=o)}$ of equation (3) drops out so that the equation of alternation in specific solvent structure of low salt concentration does not arise.

This simple treatment therefore suggests that the function $1/(N_o-N)$ may serve to straighten out the $\log\Lambda$ vs $1/(N_o-N)$ plots (Fig. 16) in the same way as the function $1/(1-\Gamma_o)$ straightened

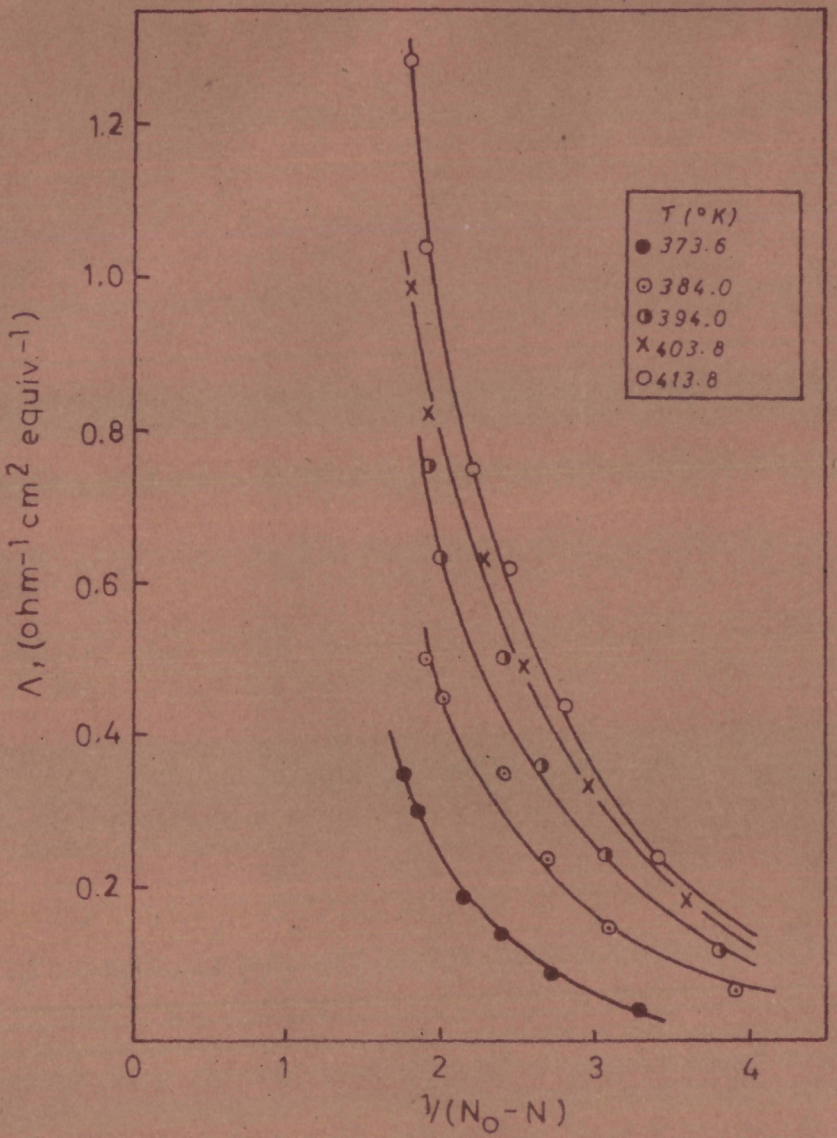

Fig. 15 Dependence of equivalent conductances, Λ on $1/(N_0-N)$ for molten mixtures of $CoCl_2$ and Bu_4NI

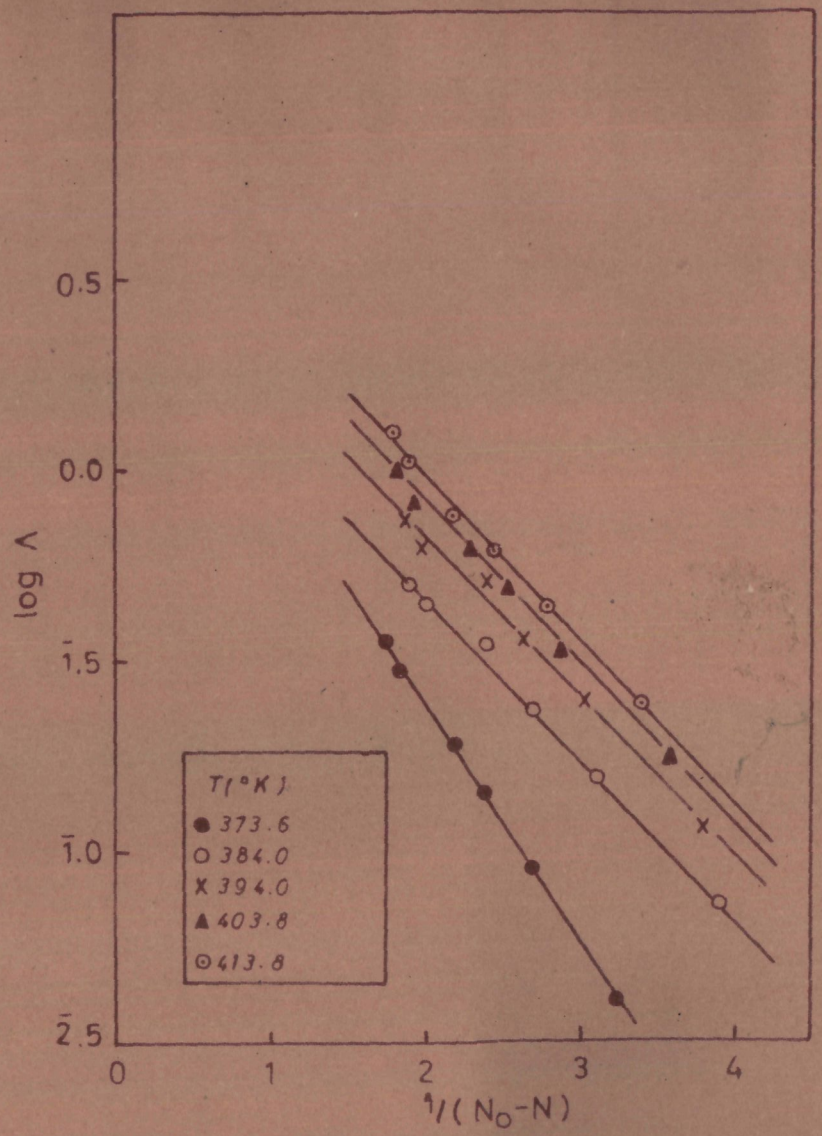

Fig. 16 Plots of log Λ vs. $1/(N_0-N)$ for molten mixtures of $CoCl_2$ and Bu_4NI.

out log k vs 1/T plots. The use of the function is subject to the same criticism noted before, viz., that it implies an additional parameter N_o, to eliminate the curvature present in the two parameter plot. The use of a third parameter seems to be convincing as it proves to have a reasonable numerical value besides an adequate theoretical justification. The values calculated from the best fit to equation (3) of the equivalent conductance data have been shown in Table IX.

The plots of Λ versus $1/(N_o-N)$ are non-linear as shown in Fig. 15. On the other hand, it may be seen from Fig. 16 that the function $1/(N_o-N)$ is capable of yielding a linear relation between log Λ and concentration which is also theoretically justified. The values of N_o giving the best linear plots at several temperatures are not very different from each other as could be expected from the standard deviation of the computed and experimental Λ values. It would be remarkable that such a simple consideration could provide a complete account of the isothermal composition dependence of conductance in such a concentrated liquid. It is also to be noted that the different values of B_Λ, A'_Λ and φ at different temperatures are not surprising. Beyond that B_Λ and φ probably remain proportional rather than constant with change in the composition. However, the observed nature of the plot (Fig. 16) justifies the validity of equation (3) for such molten salt systems.

This simple model for the conductance of concentrated

TABLE - IX

Computer fitted least square representation of $\Lambda = A_\Lambda \Sigma^{-1/2} \exp\left[\frac{-B_\Lambda}{Q(1+\alpha)}\right]$ for molten mixture of $CoCl_2$ and Bu_4NI

$[4.63 - 31.5$ mole % $CoCl_2]$

T(°K)	A_Λ	B_Λ	Q	N_o	Standard Error in Λ
373.6	71.43	-265.4	-194.3	0.6185	0.009
384.0	83.47	-155.6	-161.7	0.5698	0.02
394.0	86.07	-151.1	-161.4	0.5774	0.03
403.8	104.5	-150.7	-161.6	0.5936	0.04
413.8	134.6	-160.9	-166.1	0.6084	0.07

electrolyte solutions in which both the composition and temperature dependences of the conductance processes are considered, may also be explained in the light of configurational entropy change, ΔS_c, or the related free volume of the liquid. An adequate theory for B_Λ and f is required in order to propose a theory for concentrated ionic solutions. The theories of Adam and Gibbs[33] and Gibbs and Dimarzio[34] fulfil this requirement for transport in the liquid polymer. According to Bernal[35] and Wainwright[36], for simple molecular systems f_o should be realized at the point where the continued thermal contraction of the liquid has brought the assembly of particles to a condition of random close packing. The problem of what determines T_o may be understood from the consideration of vibrational changes in configurational degrees of freedom at T_o. The free volume model of Cohen and Turnbull suggests that T_o might be well explained in the shape of the intermolecular potential function.

Charge-transfer and the ligand-field spectra.

The charge-transfer and the ligand-field transition spectra for the tetrahedral complex ions, CoX_4^{2-} has been obtained in the thin film spectra of the glassy material of $[CoCl_2 + n\text{-}(C_4H_9)_4NI]$. An intense ultraviolet band with peaks at 32894 and 44033 cm^{-1} may be interpreted as due to the C-T processes from the nonbonding of the ligand to the antibonding

orbital of the central metal ion. The visible-near infrared band with components at 12,987(sh); 13,422; 14,984(sh); 14,388 and 15,625 cm^{-1} may be due to $^4A_2(F) \longrightarrow {}^4T_1(F)$ transitions. These components may also have some contributions from $^4A_2(F) \longrightarrow {}^4$ transition. These results are apparently similar to those reported[3] for the $CoBr_4^{2-}$ and $CoCl_4^{2-}$ complex ions in molten tetra-n-butylphosphonium bromide and chloride respectively.

ELECTRICAL CONDUCTANCE AND THE THIN FILM SPECTRA OF THE GLASSY STATES CONTAINING $CoCl_4^{2-}$, $NiCl_4^{2-}$ AND $MnCl_4^{2-}$ IN TETRA-n-BUTYLAMMONIUM CHLORIDE

Experimental

Chemicals.

Tetra-n-butylammonium chloride (Fluka AG, Switzerland) was dried in vacuum at 100°C and was used as molten salt solvent. The anhydrous manganese(II)-, cobalt(II)-, and nickel(II) chloride were prepared from their hydrated salts. The hydrated salts of Mn (E. Merck) and $NiCl_2$ (AR, BDH) were recrystallised several times from their saturated solutions prepared in triply distilled water. The hydrochloric acid gas was prepared by the laboratory method from H_2SO_4 (AR, BDH) and HCl (AR, BDH) for the preparation of anhydrous manganese(II) chloride[37].

Drying of $n\text{-}(C_4H_9)_4NCl$.

The dry box was flushed with pure dry nitrogen and then a required amount of the salt was transferred to a boiling test tube. The mouth of the tube was wrapped and tied up with a gravimetric filter paper. The tube was then placed in a double walled jacket for drying the sample in vacuum over phosphorus pentoxide (pyrex glass quickfit apparatus was used for this purpose). The vacuum dried sample was transferred to a vacuum desiccator in a dry box.

Preparation of anhydrous manganese(II) chloride[37].

The commercial manganese(II) chloride was recrystallised several times and was heated at 130°C in an atmosphere of dry hydrogen chloride gas. The salt was then ground and stored in a vacuum desiccator over phosphorus pentoxide.

Anhydrous nickel(II) chloride was prepared in the same manner as that of cobaltous chloride[22].

Procedure.

The conductance measurements were made with a conductivity bridge of Philips Type PR9500 at a frequency of 50 c/s. The concentrated solutions of tetra-n-butylammonium chloride with anhydrous manganese(II)-, cobalt(II)-, and nickel(II)-chlorides were prepared as described in the case of $CoCl_2$ and $n\text{-}(C_4H_9)_4NI$ solution. A capillary type cell (cell constant, 760.7 cm^{-1}) was used for the conductance measurements of these concentrated solutions at several temperatures with an accuracy of $\pm$ 0.03 ohm^{-1}. The conductivity cell was cleaned with hot distilled water and soaked overnight in conductivity water and the cell constant was checked after each set of measurement

The density measurements were made as described earlier in the case of molten mixtures of $CoCl_2$ and $n\text{-}(C_4H_9)_4NI$.

The concentrated solutions of n-$(C_4H_9)_4NCl$ with Mn(II)-, Co(II)-, and Ni(II)- chlorides were used in the form of thin films for recording the ultraviolet, and the visible-near infrared spectra on DK-2A recording spectrophotometer.

RESULTS AND DISCUSSION

The resistances of concentrated solutions of $MnCl_2$, $CoCl_2$ and $NiCl_2$ in $n\text{-}(C_4H_9)_4NCl$ were measured. These measurements were made over a range of temperature 373°-413°K at an interval of 5° in the cases of Mn^{2+} and Ni^{2+} while at 10 degree intervals in the case of Co^{2+}. The resistances of these concentrated solutions (i.e. glassy materials) have been measured as a function of temperature. From the specific conductance data their corresponding values of equivalent conductances were calculated with the help of the density data (Table X) which were described by the linear relations fitted by the least square method.

The Arrhenius plots for the molten $n\text{-}(C_4H_9)_4NCl + MCl_2$ (M=Mn, Co and Ni) systems have been shown in figure 17. The temperature dependence of conductance may be understood in the light of earlier discussion based on the free volume concept of ionic liquids. The equivalent conductance as well as the specific conductance data were least square fitted in different functional forms as described earlier. The typical values of the parameters for these empirical equations are given in Table XI.

The plots of $\log kT^{\frac{1}{2}}$ vs $1/(T-T_o)$ for $n\text{-}(C_4H_9)_4NCl + MCl_2$ (M=Mn, Co and Ni) molten systems have been shown in figure 18.

TABLE - X

Density and coefficient of expansion as a function of temperature for molten salt systems: $Bu_4NCl + MCl_2$ (Mn, Co and Ni)

t(°C)	$Bu_4NCl + MnCl_2$ (24.5 mole %)	$Bu_4NCl + CoCl_2$ (26.6 mole %)	$Bu_4NCl + NiCl_2$ (22.1 mole %)
	ρ (gm ml^{-1}) = 1.0413 − 0.6008 x 10^{-3} (t)	ρ (gm ml^{-1}) = 1.0425 − 0.5955 x 10^{-3} (t)	ρ (gm ml^{-1}) = 1.0496 − 0.5402 x 10^{-3} (t)
	α x 10^4	α x 10^4	α x 10^4
100	6.122	6.057	5.425
105	6.141	6.076	5.440
110	6.160	6.095	5.455
115	6.180	6.113	5.470
120	6.198	6.132	5.485
125	6.218	6.151	5.500
130	6.237	6.170	5.515
135	6.257	6.189	5.530
140	6.277	6.208	5.546

TABLE - XI

Computer fitted least square representation for specific and equivalent conductances as a function of temperature*(373°-413°K) for molten salt systems: Bu_4NCl + MCl_2(M=Mn, Co and Ni)

System	Equation No.	a	b	c	Standard Error
n-$(C_4H_9)_4NCl$ + $MnCl_2$(24.5 mole %)	(i)	0.1789×10^{-2}	-0.4223×10^{-4}	0.2622×10^{-6}	0.03
	(ii)	0.2367	923.8	243.4	0.03
	(iii)	382.5	605.1	278.5	0.006
n-$(C_4H_9)_4NCl$ + $CoCl_2$(26.6 mole %)	(i)	0.1386×10^{-2}	-0.3143×10^{-4}	0.1840×10^{-6}	0.01
	(ii)	0.0947	743.1	267.2	0.01
	(iii)	210.3	617.8	277.0	0.004
n-$(C_4H_9)_4NCl$ + $NiCl_2$(22.1 mole %)	(i)	0.0708×10^{-2}	-0.1783×10^{-4}	0.1158×10^{-6}	0.02
	(ii)	0.0851	663.63	272.10	0.02
	(iii)	160.2	621.7	271.6	0.004

(* t°C, T°K) (i) $k=a+bt+ct^2$; (ii) $k=a \exp[-b/(T-c)]$; and (iii) $\Lambda=aT^{-\frac{1}{2}} \exp[-b/(T-c)]$

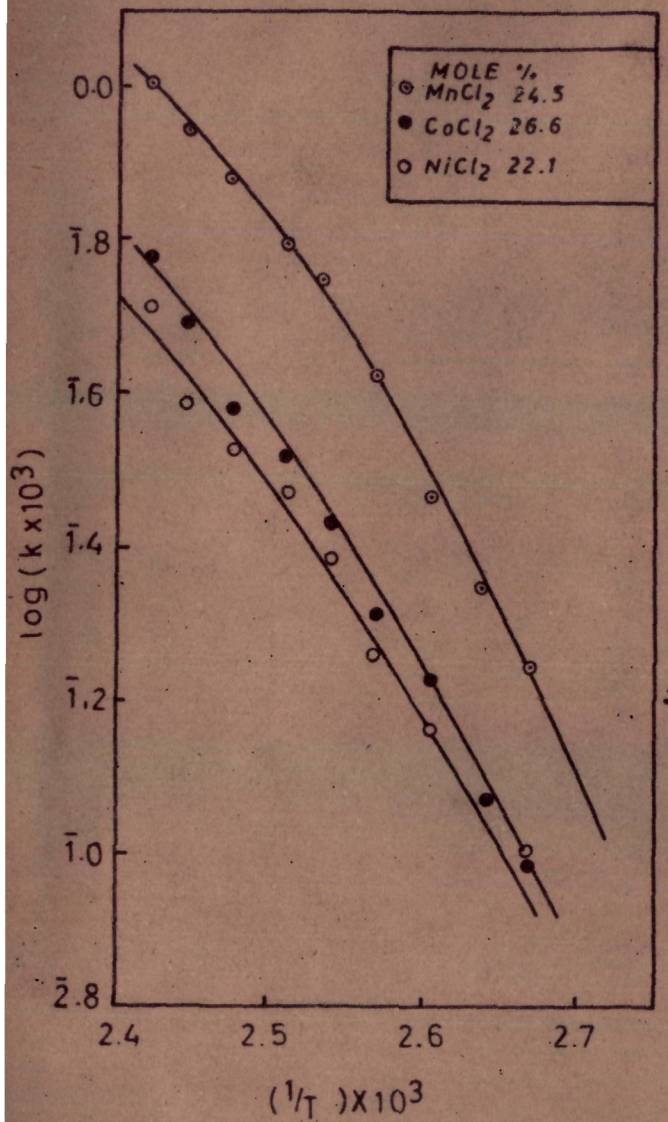

Fig. 17 Plots of $\log k$ vs. $1/T$ for molten salt system $Bu_4NCl + MCl_2$ ($M = Mn^{+2}, Co^{+2}$ & Ni^{+2})

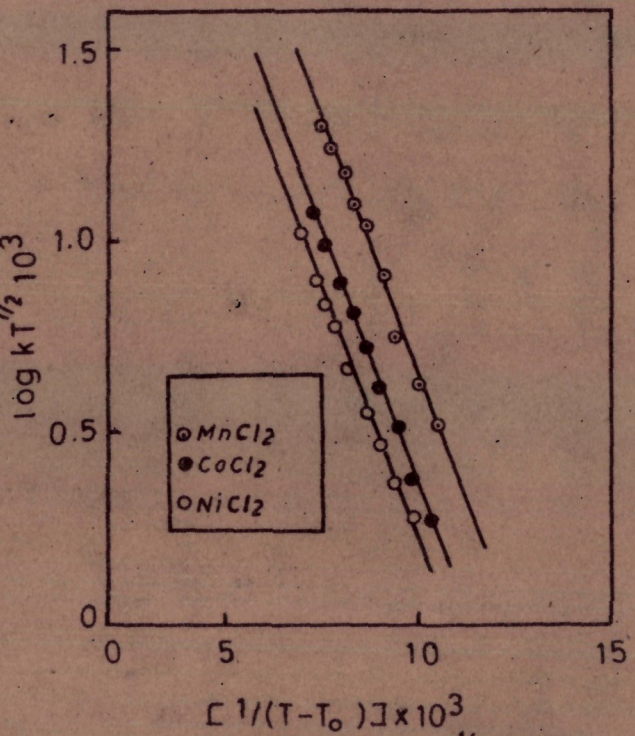

Fig. 18 Plots of $\log kT^{1/2}$ vs. $1/(T-T_o)$ for molten salt systems $Bu_4NCl + MCl_2$ ($M = Mn^{+2}, Co^{+2}$ & Ni^{+2})

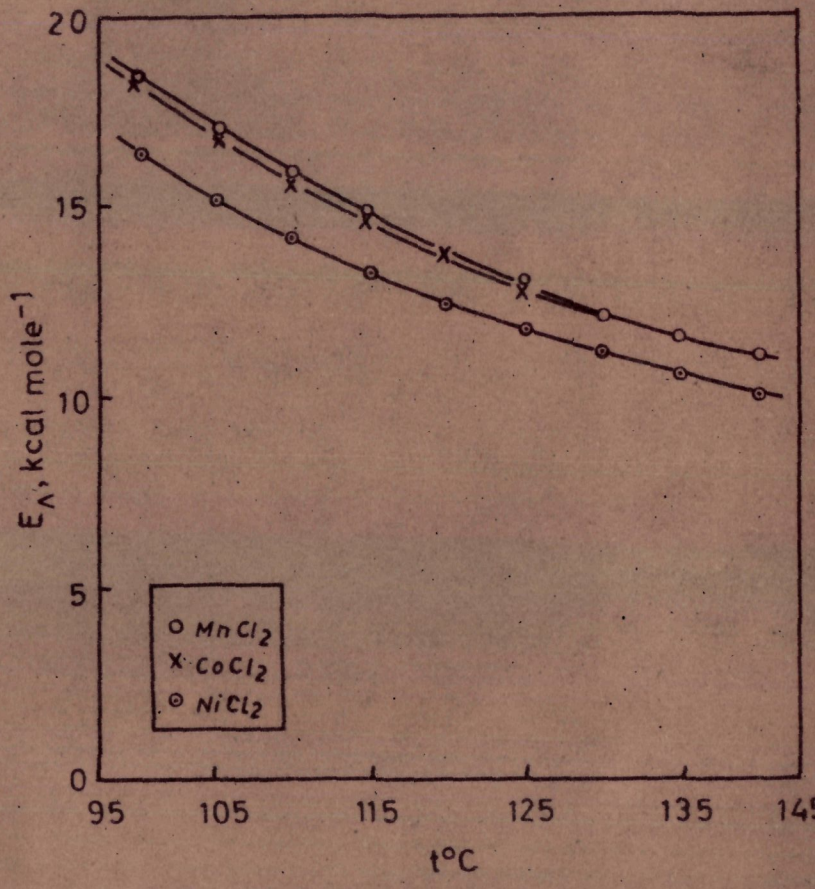

Fig. 19 Energy of activation as a function of temperature for molten salt systems $Bu_4NCl + MCl_2$ ($M = Mn^{+2}, Co^{+2}$ & Ni^{+2})

The energies of activation for equivalent conductances, E_Λ have been computed from the derivative, $\left[d\ln\Lambda/d(T^{-1})\right]$. The energies of activation E_Λ were plotted as a function of temperature as shown in figure 19. The plots, log $kT^{\frac{1}{2}}$ versus $1/(T-T_o)$ for all the three glassy materials are linear (Fig. 18) and undoubtedly confirm the appropriate choice of T_o which may be correlated with the transport behaviour of these ionic liquids. However, the temperature dependence of activation energies (Fig. 19) which could not be demonstrated in the light of Arrhenius rate process theory, could be explained in the light of free volume theory proposed by Cohen and Turnbull[10,14]. The energies of activation for specific conductances, E_k's were computed from the derivatives, $\left[d\ln k/d(T^{-1})\right]$ and also from the successive pairs of points (average 5° interval) of the Arrhenius plots, log k vs. 1/T. An average value of these activation energies, E_k's was taken to compute E_{corr} using the value of α calculated from the density data (Table X). The E_k's and E_{corr} values are given in Table XII for $MnCl_4^{2-}$, $CoCl_4^{2-}$ and $NiCl_4^{2-}$ and the plots, E_{corr} versus $\left[T/(T-T_o)\right]^2$ have been shown in figure 20. The T_o values are varied by 5° and in each case the plots have been found to pass through the origin (Fig. 20) which shows the applicability of the equation,

$$E_{corr} = A\left[T/(T-T_o)\right]^2 + B$$

TABLE - XII

Computed results of activation energy E_{corr} as a function of temperature for molten salt systems: $Bu_4NCl + MnCl_2$ (M = Mn^{+2}, Co^{+2} and Ni^{+2})

$MnCl_2 + Bu_4NCl$

t(^oK)	$\alpha RT^2 + \frac{1}{2} RT$ (kcal/mole)	E_k^1	E_k^2 (kcal/mole)	E_k^3	E_{corr} (kcal/mole)
373	0.540	15.02	15.20	15.99	15.95
378	0.550	14.84	14.47	14.47	15.27
383	0.560	14.25	13.81	13.71	14.48
388	0.570	13.52	13.21	12.80	13.74
393	0.580	12.78	12.66	12.56	13.24
398	0.591	12.09	12.16	12.17	12.73
403	0.601	11.47	11.70	11.42	12.13
408	0.612	10.91	11.27	10.65	11.55
413	0.623	10.41	10.88	10.28	11.14

* E_k^1, from the derivative of $a+bt+ct^2$; E_k^2 ; from the derivative of $a \exp[-b/(T-c)]$, and E_k^3 ; from the slope of Arrhenius plot, log k vs. 1/T.

TABLE - XII (Contd.)

$CoCl_2$ + Bu_4NCl

t(°K)	$\alpha RT^2 + \frac{1}{2} RT$ (kcal/mole)	ε_k^1	ε_k^2 (kcal/mole)	ε_k^3	ε_{corr} (kcal/mole)
373	0.538	17.97	18.33	16.28	18.73
378	0.548	17.95	17.17	16.72	17.63
383	0.558	17.06	16.14	15.22	16.70
388	0.568	15.92	15.22	14.85	15.90
393	0.578	14.82	14.40	13.71	14.89
398	0.589	13.82	13.66	12.79	14.01
403	0.599	12.93	12.99	11.42	13.04
408	0.610	12.17	12.39	10.81	12.30
413	0.621	10.50	11.84	9.69	11.29

TABLE - XII(Contd.)

$NiCl_2$ + Bu_4NCl

t(°K)	$\alpha RT^2 + \frac{1}{2} RT$ (kcal/mole)	ε_k^1	ε_k^2 (kcal/mole)	ε_k^3	ε_{corr} (kcal/mole)
373	0.521	17.79	18.02	18.28	18.55
378	0.530	16.39	16.80	17.37	17.38
383	0.540	15.08	15.73	15.99	16.14
388	0.550	13.94	14.78	14.85	15.07
393	0.559	12.96	13.94	13.71	14.20
398	0.569	12.13	13.18	12.80	13.40
403	0.579	11.41	12.49	11.99	12.70
408	0.588	10.80	11.19	11.43	12.04
413	0.598	10.27	11.33	10.65	11.30

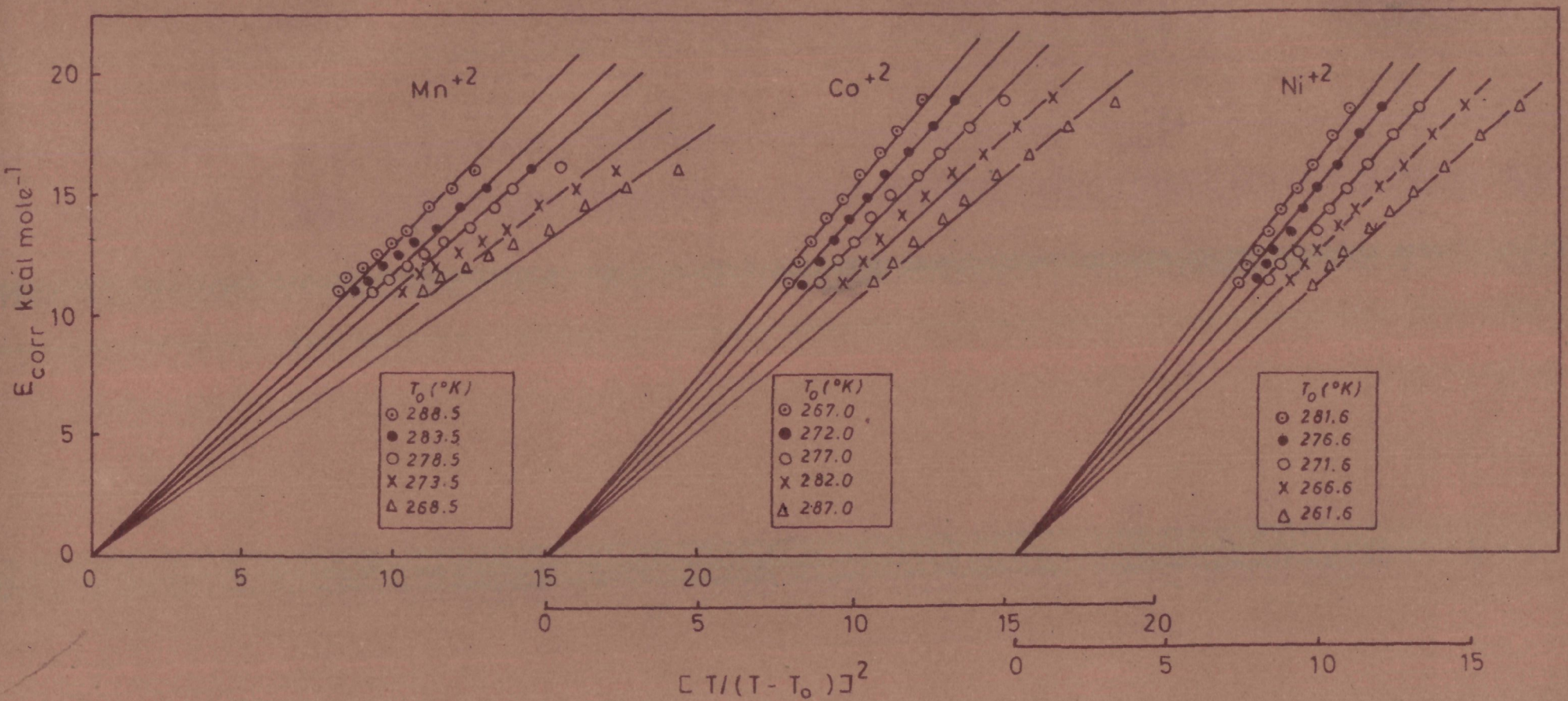

Fig. 20 Test of results for sensitivity to T_o of E_{corr} vs. $[T/(T-T_o)]^2$ plots for molten salt systems: $Bu_4NCl + MCl_2$ ($M = Mn^{+2}$, Co^{+2} & Ni^{+2})

and at the same time justifies the appropriate choice of T_e values as may be seen from Table XI. It is seen that the electrical conductances keep on decreasing from manganese through nickel which in turn justifies the decrease in the corresponding T_e values from Mn^{2+} to Ni^{2+}. The lower values of conductance with an increase in the concentration of MCl_2 (M=Mn, Co and Ni) may also be interpreted as due to the complex formation which may be supported on the basis of their spectral studies.

Spectra of the thin films of glassy states containing $CoCl_4^{2-}$, $NiCl_4^{2-}$ and $MnCl_4^{2-}$ in tetra-n-butylammonium chloride.

The spectra consist of an intense band in the visible-near infrared regions arising from the $3d^n \longrightarrow 3d^n$ ligand-field transitions and relatively much stronger bands in the ultraviolet region due to the charge-transfer processes.

The spectrum of the concentrated solution of $CoCl_2$ in $n\text{-}(C_4H_9)_4NCl$ consists of an intense band with peaks at 234 and 217 mμ (42,735 and 46,083 cm^{-1}) in the ultraviolet region and comparatively less intense band with structure is located between 600-800 mμ (14,490; 15,150; 16,000 and 16,390 cm^{-1}).

The molten salt spectra resemble that of the room temperature crystal spectrum of Co(II) ion obtained by isomorphous

substitution of Zn(II) ion in Cs_2ZnCl_4 lattice in which Zn(II) ions are presumably surrounded tetrahedrally by chloride ion, proves the presence of tetrahedral geometry in molten salts. The chloride and bromide spectra are very much alike except that in the latter case the bands are shifted towards lower energy side. Our spectra resemble with those reported by Sundheim and Islam[3] for the tetrahedral $CoCl_4^{2-}$ and $CoBr_4^{2-}$ in molten R_4PX (X=Cl, Br).

Ligand-field transitions.

Three transitions are spin-allowed[38], two of which are orbital transitions due to the splitting of the ground state term ^4F by the tetrahedral field into $^4A_2$, $^4T_1$ and $^4T_2$ irreducible representations, and the third one is from the ground $^4A_2(F)$ term to the first excited state $^4T_1(P)$[38-40], out of these two, $^4A_2(F) \longrightarrow {}^4T_2(F)$ and $^4A_2(F) \longrightarrow {}^4F_1(F)$ transitions, the first is forbidden for electrical dipole absorption in pure tetrahedral geometry[41] although reported as a weak band at 2900 cm^{-1} in $(Et_4N)_2CoBr_4$ in an organic solvent[42]. These two transitions were not recorded in thin film spectra because of their low intensity values.

The intense resolved band which lies between 600-800 mμ may be assigned as due to $^4A_2(F) \longrightarrow {}^4T_1(P)$ transitions although some of the peaks have also contributions from a few of the spin

forbidden doublets, ^2G as discussed by Sundheim and Islam[3]. A comparison of our results with those reported earlier may support our conclusion that the absorbing species in molten Bu_4NX (X=Cl, I) in dilute as well as in the corresponding concentrated solutions which supercool to glassy states remain tetrahedral.

$(Et_4N)_2CoBr_4$ in CH_3NO_2[43]	$(Bu_4N)_2CoBr_4$ in CH_2Cl_2[44]	$(Bu_4P)_2CoBr_4$ melt[3]	$(Bu_4P)_2CoCl_4$ melt[3]	$(Bu_4N)_2CoCl_4$ melt
13,830 cm^{-1}(Sh)	13,740 cm^{-1}	13,736 cm^{-1}	14,369 cm^{-1}	14,490 cm^{-1}
14,327 ,,	14,290 ,,	14,245 ,,	14,969 ,,	15,150 ,,
14,970 ,,	14,950 ,,	15,000 ,,	15,873 ,,	16,000 ,,
15,804 ,,	15,600 ,,	15,552 ,,	16,295 ,,	16,390 ,,

Charge-transfer spectra.

It has been shown by Craig, et al.[45] that the term value differences are strongly altered by the effects of outer screening when orbital expansion is included. They have also pointed out that the effect of 4d covalency in octa- and tetra-hedral metal complexes are important and that partial $4s\ 4p^3$ covalent bonding is probable for $CoCl_4^{2-}$ but unlikely for octahedral complex. If this is so, then the molecular orbitals which are mainly ligand in character will be relatively more bonding for tetrahedral

complex and the energy difference between these and the metal 3d orbitals will be increased for the tetrahedral over that for the octahedral complex. The charge-transfer band should therefore lie at lower energies in octahedral than in tetrahedral inspite of the large splitting of the 3d orbitals, if the amount of 4d covalency is at all appreciable in tetrahedral complexes.

A number of measurements have been made in organic solvents[42,43,46-48], in crystals[38,49,50] and few[51,52] in molten salts containing tetrahedral CoX_4^{2-} (X=Cl, Br, I), but the charge transfer spectra has not been reported in these media[43,44,46,52] except one in molten Bu_4PX (X=Cl, Br)[2]. The reason for not obtaining a charge-transfer band in CoX_4^{2-} was purely due to experimental difficulties[3], for example in crystals containing $CoCl_4^{2-}$, a relatively much higher chloride concentration in the host lattice seems to mask the charge-transfer band as the charge-transfer band of the host chloride is presumably located near those of the $CoCl_4^{2-}$ complex ion. Similarly in organic solvents, the relatively higher solvent halide ion concentrations and the longer path lengths of the cells seem to be the reason for not obtaining such a band in these media[3].

A comparison[2,3] of the spectra of thin films of the glassy states containing $CoCl_4^{2-}$ ions support our conclusion that the band with peaks at 42,735 and 46,083 cm^{-1} are due to charge-transfer processes. Thus the presence of an appreciable covalent

character supports the presence of a charge-transfer band in CoX_4^{2-}

$NiCl_4^{2-}$

The thin film spectrum of $NiCl_2$ in molten n-$(C_4H_9)_4NCl$ consists of an intense band with maxima at 35,460; 38,460 and 42,550 cm^{-1} in the UV region and an intense band with peaks at 14,282; 15,385; and a shoulder at 16,475 cm^{-1} in the visible-infrared regions.

An excellent agreement between the spectrum of $NiCl_2$ in molten n-$(C_4H_9)_4NCl$ and those reported by Smith et al[54] supports the view that the present solvent favours tetrahedral structure for the metal complex ions.

The band with peaks at 14,285; 15,385 and a shoulder at 16,475 cm^{-1} may be assigned to $^3T_1(F) \longrightarrow {}^3A_2(F)$ transitions as reported earlier[3,54].

	$NiCl_4^{2-}$ in $(CH_3)_2SO_2$+LiX[54]	$NiCl_4^{2-}$ in Bu_4NaPCl[54]	$NiCl_4^{2-}$ in Bu_4PCl[3]	$NiCl_4^{2-}$ in Bu_4NCl
L-F.	14,160 cm^{-1}	14,140 cm^{-1}	14,160 cm^{-1}	14,285 cm^{-1}
	15,810 ,,	15,370 ,,	15,367 ,,	15,385 ,,
	16,300(sh)	16,200(sh)	16,393(sh)	16.475 ,,
C-T.	35,840 ,,	-	-	35,460 ,,
	38,760 ,,	-	-	38,460 ,,
	42,100(sh)	-	-	42,550 ,,
	43,100 ,,	-	-	

The band with maxima at 35,460; 38,460 and 42,550 cm^{-1} in the ultraviolet region may be assigned as due to the charge-transfer processes in tetrahedral $NiCl_4^{2-}$ complex ion from the non-bonding orbital of the ligand to that of the antibonding of the central metal ion. A comparison of our results with those reported earlier[3,54] supports our conclusion that the metal complex ion has T_d geometry.

$MnCl_4^{2-}$

The absorption spectra of tetrahedral tetrahalomanganese(II) complex ions have been studied in organic solvents[53,55-57], molten salts[52], as well as in solid state[58]. The present work deals with the absorption spectra of thin films of the glassy material ($MnCl_2$-rich mixtures of $n\text{-}(C_4H_9)_4NCl$).

The $3d^5 \longrightarrow 3d^5$ ligand-field transition bands belong to the weak-field case in which the ground state has been derived from the $^6A_1(S)$ state of the free ion. The intensities of the ligand-field transition bands are very low as all the transitions are spin-forbidden. The intensity is much greater for tetrahedral geometry than those for octahedral as the former has no centre of symmetry. The absorption bands for T_d complexes are generally found to be more intense than those for octahedral. This fact has been used as a criterion to distinguish between tetrahedral and an octahedral configurations. This is in accord

with the operation of the Laporte's selection rule[59].

The thin film spectra of $MnCl_4^{2-}$ in n-$(C_4H_9)_4NCl$ consists of a band at 37,736 cm^{-1} (265 mμ) which may be assigned as due to the charge-transfer processes (also presumably covering the components of the ^4P term). As the ligand-field transitions are forbidden, the weak bands have not been recorded in the thin film.

$(Bu_4P)_2MnBr_4$ in melt[3]	$MnCl_4^{2-}$[53]	$(Et_4N)_2MnBr_4$[56]	$(Bu_4N)_2MnCl_4$ in melt.
36,360 cm^{-1}	37,100 cm^{-1}	36,200 cm^{-1}	37,736 cm^{-1}

A comparison of this band in the ultraviolet region with those reported earlier[3,53,56] may support our conclusion that the absorbing species in $MnCl_2$-rich mixtures of molten n-$(C_4H_9)_4NCl$ is tetrahedral.

APPENDIX

A. Calculation of equivalent conductance.

From the specific conductance data, equivalent weight, e, and the density ρ, the equivalent conductance, that is, the conductance of one equivalent of electrolyte between parallel electrodes 1 cm apart, was calculated using the equation established by Harry Bloom[60].

$$\Lambda = \frac{ke}{\rho} = k V_e \quad \text{----------} \quad (1)$$

where V_e ml = equivalent volume of the molten salt.

For mixtures of molten salts

$$\Lambda = \frac{k\bar{e}}{\rho} \quad \text{----------} \quad (2)$$

where $\bar{e}$ = mean equivalent weight calculated from the equation

$$\bar{e} = f_1 e_1 + f_2 e_2 \quad \text{----------} \quad (3)$$

where f_1 and f_2 are the equivalent fractions of component 1 and 2 respectively and e_1 and e_2 are their corresponding equivalent weights.

For g_1 gm of $MnCl_2$ mixed with g_2 gm of $n\text{-}(C_4H_9)_4NX$ (X=Cl, Br and I), the equivalent fractions are

$$f_{MnCl_2} = \frac{\dfrac{g_1}{\text{Eq.wt. of } MnCl_2}}{\dfrac{g_1}{\text{Eq.wt. of } MnCl_2} + \dfrac{g_2}{\text{Eq.wt. of } Bu_4NX}} \quad \text{------ (4)}$$

and

$$f_{Bu_4NX} = \frac{\dfrac{g_2}{\text{Eq. wt. of } Bu_4NX}}{\dfrac{g_1}{\text{Eq.wt. of } MnCl_2} + \dfrac{g_2}{\text{Eq.wt. of } Bu_4NX}} \quad \text{------ (5)}$$

Thus for $MnCl_2$, the expression (4) may be modified as

$$f_{MnCl_2} = \frac{\dfrac{2g_1}{M_{MnCl_2}}}{\dfrac{2g_1}{M_{MnCl_2}} + \dfrac{g_2}{M_{Bu_4NX}}} = \frac{2n_{MnCl_2}}{2n_{MnCl_2} + n_{Bu_4NX}} \quad \text{-- (6)}$$

where the M's are the molecular weights and n's the number of moles. If x be the mole fraction of $MnCl_2$ mixed with (1-x) mole fraction of Bu_4NX, then

$$x = \frac{n_{MnCl_2}}{n_{MnCl_2} + n_{Bu_4NX}} \text{ ; and } (1-x) = \frac{n_{Bu_4NX}}{n_{MnCl_2} + n_{Bu_4NX}}$$

$$\therefore \quad \frac{x}{(1-x)} = \frac{n_{MnCl_2}}{n_{Bu_4NX}} \quad \text{---------- (7)}$$

Substituting equation (7) into equation (6), we get

$$f_{MnCl_2} = \frac{2x}{2x + (1-x)} \quad \text{---------- (8)}$$

Similarly for Bu_4NX

$$f_{Bu_4NX} = \frac{(1-x)}{2x + (1-x)} \quad \text{----------(9)}$$

Thus the equation for mean equivalent weight, $\bar{e}$ may be written as

$$\bar{e} = f_1 e_1 + f_2 e_2$$

$$\therefore \quad \bar{e} = \frac{2xe_1}{2x + (1-x)} + \frac{(1-x)e_2}{2x + (1-x)} \quad \text{-------(10)}$$

For each mole fraction of $MnCl_2$ the mean equivalent weight, $\bar{e}$ was calculated with the help of equation (10).

B. Calculation of energy of activation.

(a) The energy of activation for specific conductance, E_k was calculated from the derivatives of the following empirical equations.

$$k = a + bt + ct^2 \quad \text{----------(11)}$$

and $$k = a' \exp\left[-b'/(T-c')\right] \quad \text{----------(12)}$$

where k is the specific conductance, a, b, and c and a', b' and c' are the parameters of the respective equations and t(^oC) and T(^oK) stand for the temperature.

The equation (11) may be written as

$$k = a + b\,(T-273) + c(T-273)^2$$

Taking its logarithm and differentiating with respect to T we have

$$\ln k = \ln \left[a + b\,(T-273) + c\,(T-273)^2 \right]$$

$$\frac{d\ln k}{dT} = \left[\frac{b + 2c\,(T-273)}{a + b(T-273) + c\,(T-273)^2} \right]$$

Since $\frac{d\ln k}{d(1/T)} = -T^2 \left(\frac{d\ln k}{dT} \right)$ we have,

$$\frac{d\ln k}{d(1/T)} = -\frac{E_k}{R} = -T^2 \left[\frac{b + 2c\,(T-273)}{a+b\,(T-273) + c(T-273)^2} \right]$$

$$\therefore \quad E_k = \left[\frac{b + 2c\,(T-273)}{a+b\,(T-273) + c\,(T-273)^2} \right] T^2 \times R$$

(b) Similarly by differentiating the logarithm of equation (12) we have the derivative $\left[d\ln k / d\,(T^{-1}) \right]$ as

$$\frac{d\ln k}{dT} = \frac{b'}{(T-c')^2}$$

Since $\frac{d\ln k}{d(1/T)} = -T^2 \frac{d\ln k}{dT}$

Therefore, we have

$$\frac{d\ln k}{d(1/T)} = -T^2 \frac{b'}{(T-c')^2} = -\frac{E_k}{R}$$

$$\therefore \quad E_k = T^2 \frac{b'}{(T-c')^2} \times R$$

(c) The energy of activation for equivalent conductance, E_Λ was calculated from the derivative, $\left[d\ln\Lambda/d(T^{-1})\right]$. Thus the equation for equivalent conductance is

$$\Lambda = AT^{-\frac{1}{2}} \exp\left[-k_\Lambda/(T-T_0)\right] \text{ - - - - - - - - - - - - - (13)}$$

Taking logarithm and differentiating with respect to T, we get

$$\frac{d\ln\Lambda}{dT} = -\left[1/2T - k_\Lambda/(T-T_0)^2\right]$$

$$= -\left[k_\Lambda/(T-T_0)^2 - 1/2T\right]$$

Since $\left[d\ln\Lambda/d\ (T^{-1})\right] = -T^2 \ \frac{d\ln\Lambda}{dT}$, we have

$$\frac{d\ln\Lambda}{d(1/T)} = -\left[k_\Lambda/(T-T_0)^2 - 1/2T\right] \times T^2$$

$$\therefore \quad E_\Lambda = \left[k_\Lambda/(T-T_0)^2 - 1/2T\right] \times T^2 \times R$$

C. <u>Calculation of coefficient of cubical expansion, α:</u>
The coefficient is defined as

$$\alpha = (1/V_0)(\partial V/\partial T)_p \text{ - - - - - - - - - - - - - (14)}$$

where V_0 is the initial volume and α has got the dimension of 1/T. The density data has been fitted in the form

$$\rho = a - bt \text{ - - - - - - - - - - - - - - - - - (15)}$$

where a and b are constants of the linear plot. From equation

(15) one may obtain the value of α as

$$M/V = a - bt \text{ or } a-bT$$

Differentiating with respect to T, we get

$$-M/V^2 = - b dT$$

$$\text{or } (1/V)(\partial V/\partial T)_p = (V/M)b \qquad (V_o \approx V)$$

$$\therefore (1/V)(\partial V/\partial T)_p = (1/\rho)b$$

Therefore $\alpha = b/(a - bt)$ or $\alpha = b/(a - bT)$

D. <u>Computation of E_{corr} values</u>.

The fundamental equation for diffusion and equivalent conductances are

$$D = A_D T^{\frac{1}{2}} \exp\left[-k_D/(T-T_o)\right] \text{ - - - - - - - - - - (16)}$$

and $$\Lambda = A_\Lambda T^{-\frac{1}{2}} \exp\left[-k_\Lambda/(T-T_o)\right] \text{ - - - - - - - - - (17)}$$

From equation (16), a corrected energy of activation E_{corr} has been defined[1,18] as

$$E_{corr} = E_D - 1/2\ RT = k_D R\left[k_D/(T-T_o)\right] \text{ - - - (18)}$$

Using Nernst-Einstein equation, one derives:

$$E_D = E_\Lambda + RT \text{ - - - - - - - - - - - - - - (19)}$$

The energy of activation for equivalent and specific conductances are related through the equation

$$E_{\Lambda} = E_{k} + \alpha RT^{2} \text{ - - - - - - - - - - - - - - - - (20).}$$

where α is the coefficient of expansion for the melt. Thus E_{corr} can be obtained by substituting equations (19) and (20) in equation (18).

$$E_{corr} = E_{k} + \alpha RT^{2} + RT - (1/2)\,RT$$

$$= k_{\Lambda} R \left[T/(T-T_{o})\right]^{2}$$

$$E_{corr} = E_{k} + \alpha RT^{2} + \tfrac{1}{2}RT = k_{\Lambda} R \left[T/(T-T_{o})\right]^{2}$$

E. <u>Measurements of capacitance of the electrical double layer (electrode-electrolyte) of 31.5 mole % $CoCl_2$ + n-$(C_4H_9)_4NI$ melt.</u>

The dielectric constant of the melt has been calculated from the calibration curve made with the following standard liquids.

Liquids	Dielectric constant ϵ	Instrument Response
Water	80.37	22,350
Methanol	32.63	17,022
Quinoline	9.00	8,485
Benzene	2.28	1,720
Acetone	20.70	14,242
Chloroform	4.81	4,400
Ethanol	24.30	16,000
Acetyl chloride	16.90	12,308
Nitrobenzene	34.82	17,360
Molten salt $CoCl_2$(31.5 mole %) + n-$(C_4H_9)_4NI$	5.5 (calc.)	5,005

The capacitance of the electrical double layer may be defined as[24]

$$C' = \frac{10^9 \epsilon}{4\pi c^2 (l/A)}$$

where ϵ = dielectric constant

c = velocity of light, and

l/A = Cell constant

(a) For cell of cell constant value 1.028 cm^{-1} at a frequency of 50 c/s, the capacitance is $C' \cong 1.42$ picofarads.

The corresponding magnitude of impedence = $1/2\pi fC' \cong 2.28 \times 10^9$ ohm.

(b) For cell of cell constant value 1612 cm^{-1}, the capacitance

$$C' \approx 3.022 \times 10^{-4} \text{ picofarads}$$

Impedence = $1/2 \pi fC' \cong 1.05 \times 10^{13}$ ohm .

(c) For cell of cell constant value 760 cm^{-1}, the capacitance

$$C' \approx 6.3 \times 10^{-4} \text{ picofarads}$$

Impedence = $1/2 \pi fC' \cong 5.05 \times 10^{12}$ ohm.

BIBLIOGRAPHY

1. C.A. Angell, J. Phys. Chem., 68, 1917 (1964).

2. B.R. Sundheim and N. Islam, Appl. Spectroscopy (In press).

3. N. Islam, doctoral dissertation, New York University, 1968 (DA XXIX, 966-B; University Microfilms, Ann Arbor, Mich., No. 68-13, 122).

4. G. Pedro Smith and S. von Winbush, J. Am. Chem. Soc., 89, 2127 (1966).

5. A.J. Easteal and I.M. Hodge, J. Phys. Chem., 74, 730 (1970).

6. G.J. Janz, J. Chem. Ed., 39, 59 (1962).

7. G.J. Janz, C. Solomons, and M.J. Gardner, Chem. Rev., 58, 461 (1958).

8. H. Bloom, Rev. Pure and Appl. Chem., 9, 139 (1959).

9. H. Bloom and J.O.M. Bockris, 'Modern Aspects of Electrochemistry', No. 2, Academic Press, Inc., N.Y. (1959).

10. M.H. Cohen and D. Turnbull, J. Chem. Phys., 31, 1164 (1959).

11. M.R. Islam, Dissertation submitted for the partial fulfilment of the requirements of the degree of Master of Philosophy in Chemistry to the Aligarh Muslim University (1970); 'Electrical conductance and the glass-forming tendency of molten salt mixtures of manganese(II) chloride and tetra-n-butylammonium halide', N. Islam and M.R. Islam, communicated to Z. Phys. Chem. (Leipzig).

12. E.R. Van Artsdalen, and I.S. Yaffe, J. Phys. Chem., 59, 118 (1955); I.S. Yaffe and E.R. Van Artsdalen, ibid., 60, 1125 (1956).

13. J.O'M. Bockris, E.H. Crook, H. Bloom, and N.E. Richards, Proc. Roy. Soc., A255, 558 (1960).

14. D. Turnbull and M.H. Cohen, J. Chem. Phys., 34, 120 (1961).

15. H. Bloom, J.W. Knaggs, J.J. Molloy, and D. Welch, Trans. Faraday Soc., 49, 1458 (1953).

16. F.H. Stillinger, J.G. Kirkwood, and P.J. Wolfwicz, J. Chem. Phys., 32, 1837 (1960).

17. C.A. Angell, J. Phys. Chem., 68, 218 (1964).

18. H.C. Gaur and S.K. Jain, Revue Roumaine de Chimie, 16, 8, 1157-1163 (1971); H.C. Gaur and S.K. Jain, Indian J. Chem., 9, 860 (1971).

19. S.A. Rice, Trans. Faraday Soc., 58, 499 (1962).

20. D.F. Evans, C. Zawoyski, and R.L. Kay, J. Phys. Chem., 69, 3878 (1965).

21. I. Vogel, 'Text Book of Practical Organic Chemistry', 3rd Edition, Longmans, Green and Co., London, pp. 171, 183, 189 (1924).

22. T. Moeller, 'Inorg. Synthesis', Vol. V, p. 153, McGraw-Hill Book Co., Inc., New York (1957).

23. E.W. Washburn, 'International critical tables of numerical data, Physics, Chemistry and technology', Vol. III, McGraw-Hill Book Co., Inc., New York, p. 29, (1928).

24. J. Braunstein and G.D. Robbin, J. Chem. Ed., 48, 52 (1971).

25. C.A. Angell, J. Phys. Chem., 70, 3988 (1966); 70, 2793 (1966).

26. C.A. Angell, Aust. J. Chem., 23, 929 (1970).

27. C.T. Moynihan, J. Phys. Chem., 70, 3399 (1966).

28. C.T. Moynihan et al., J. Phys. Chem., 73, 3287 (1969).

29. E.R. Nightingale, Jr., J. Phys. Chem., 63, 1381 (1959).

30. A.A. Miller, J. Polymer Sci., A1, 1857 (1963).

31. G.S. Fulcher, J. Am. Ceram. Soc., 8, 339 (1925).

32. M.L. Williams, R.F. Landel, and J.D. Ferry, J. Am. Chem. Soc., 77, 3701 (1955).

33. G. Adam and J.H. Gibbs, J. Chem. Phys., 43, 139 (1965).

34. J.H. Gibbs and E.A. Dimarzio, J. Chem. Phys., 28, 373 (1958).

35. J.D. Bernal and J. Mason, Nature, 188, 910 (1960).

36. B.J. Alder and T.E. Wainwright, J. Chem. Phys., 31, 459 (1959)

37. J.H. Kleinhekscl and H.C. Kremers, J. Am. Chem. Soc., 50, 959 (1928).

38. J. Ferguson, J. Chem. Phys., 39, 116 (1963).

39. J.S. Griffith, Theory of Transition-Metal Ions, Cambridge University Press, Cambridge, 1961, p. 80.

40. C.J. Ballhausen, 'Introduction to Ligand-Field Theory', McGraw-Hill Book Company Inc., New York, N.Y., 1962, p. 253.

41. A.D. Liehr and C.J. Ballhausen, J. Mol. Spectroscopy, 2, 342 (1958); 4, 190 (1960).

42. P. Ros, Rec. Trav. Chim., 82(8), 823-7 (1963).

43. N.S. Gill and R.S. Nyholm, J. Chem. Soc., 3997 (1959).

44. F.A. Cotton, D.M.L. Goodgame, and M. Goodgame, J. Am. Chem. Soc., 83, 4690 (1961).

45. D.P. Craig and E.A. Magnusson, Disc. Faraday Soc., 26, 116 (1958).

46. F.A. Cotton and M. Goodgame, J. Am. Chem. Soc., 83, 1777 (1961).

47. C.J. Ballhausen and C.K. Jørgensen, Acta Chem. Scand., 9, 397 (1955).

48. R.H. Holm and F.A. Cotton, J.Chem. Phys., 31, 788 (1959).

49. H.A. Weakliem, J. Chem. Phys., 36, 2117 (1962).

50. A. Trutia and M. Voda, Phys. Status Solidi, 15(1), K27-K29 (1961).

51. D.M. Gruen and R.L. McBeth, Pure Appl. Chem., 6, 23 (1963).

52. B.R. Sundheim and M. Kukk, Disc. Faraday Soc., 32, 49 (1961).

53. S. Buffagnie and T.M. Dunn, Nature, 186, 937 (1960).

54. G.P. Smith, C.H. Liu, and T.R. Griffiths, J. Am. Chem. Soc., 86, 4796 (1964).

55. R.S. Nyholm, J. Chem. Soc., 3997 (1963).

56. F.A. Cotton, D.M.L. Goodgame, and M. Goodgame, J. Am. Chem. Soc., 84, 167 (1962).

57. D.M.L. Goodgame and F.A. Cotton, J. Chem. Soc., 3735 (1961).

58. C.K. Jørgensen, Acta Chem. Scand., 11, 53 (1957).

59. R. Englman, Mol. Phys., 3, 48 (1960).

60. H. Bloom, 'The Chemistry of Molten Salts', P. 80, W.A. Benjamin, Inc., N.Y. (1967).